Final Technical Progress Report for Project Entitled "Impact of DME-Diesel Fuel Blend Properties on Diesel Fuel Injection Systems"

May 16, 2001-February 15, 2004

Elana M. Chapman, Andre Boehman, Kimberly Wain,
Wallis Lloyd, Joseph M. Perez, Donald Stiver, Joseph Conway

Report Issue Date:
April 2004

DOE Award Number: DE-FC26-01NT41115

The Pennsylvania State University
The Energy Institute
University Park, PA 16802

DISCLAIMER

ABSTRACT

The objectives of this research program are to develop information on lubricity and viscosity improvers and their impact on the wear mechanisms in fuel injectors operating on blends of dimethyl ether (DME) and diesel fuel. Since DME is a fuel with no lubricity (i.e., it does not possess the lubricating quality of diesel fuel), conventional fuel delivery and fuel injection systems are not compatible with dimethyl ether. Therefore, to operate a diesel engine on DME one must develop a fuel-tolerant injection system, or find a way to provide the necessary lubricity to the DME. In the shuttle bus project, we have chosen the latter strategy in order to achieve the objective with minimal need to modify the engine. Our strategy is to blend DME with diesel fuel, to obtain the necessary lubricity to protect the fuel injection system and to achieve low emissions. In this project, we have sought to develop methods for extending the permissible DME content in the DME-diesel blends without experiencing rapid injector failure due to wear.

Our activities have covered three areas: examination of the impact of lubricity additives on the viscosity of DME, development of a high-pressure lubricity test apparatus for studies of lubricity and viscosity improvers and development of an injector durability stand for evaluation of wear rates in fuel injectors. The first two of these areas have resulted in valuable information about the limitations of lubricity and viscosity additives that are presently available in terms of their impact on the viscosity of DME and on wear rates on injector hardware. The third area, that of development of an injector durability test stand, has not resulted in a functioning experiment. Some information is provided in this report to identify the remaining tasks that need to be performed to make the injector stand operational.

The key observations from the work are that when blended at 25 wt.% in either diesel fuel or Biodiesel fuel, DME requires more than 5 wt.% additive of all viscosity and lubricity additives tested here to even approach the lower limit of the ASTM diesel fuel viscosity requirement. To treat neat DME sufficiently to make DME comply with the ASTM diesel fuel viscosity requirement would require a viscosity additive with 10^{45} cSt viscosity, which is not possible with current additive technologies.

TABLE OF CONTENTS

LIST OF FIGURES

EXECUTIVE SUMMARY

The objectives of this research program are to develop information on lubricity and viscosity improvers and their impact on the wear mechanisms in fuel injectors operating on blends of dimethyl ether (DME) and diesel fuel. This project complements another recently completed project titled "Development of a Dimethyl Ether (DME)-Fueled Shuttle Bus Demonstration Project," under agreement #DE-FG29-99FT40161. The objectives of that research and demonstration program are to convert a campus shuttle bus to operation on dimethyl ether, a potential ultra-clean alternative diesel fuel. Since DME is a fuel with no lubricity (i.e., it does not possess the lubricating quality of diesel fuel), conventional fuel delivery and fuel injection systems are not compatible with dimethyl ether. In the shuttle bus project, we chose the strategy of trying to improve the viscosity of DME in order to achieve the objective with minimal need to modify the engine. Our strategy is to blend DME with diesel fuel, to obtain the necessary lubricity to protect the fuel injection system and to achieve low emissions. In this project, we have sought to develop methods for extending the permissible DME content in the DME-diesel blends without experiencing rapid injector failure due to wear.

To date, our activities have covered three areas: examination of the impact of lubricity additives on the viscosity of DME, development of a high-pressure lubricity test apparatus for studies of lubricity and viscosity improvers and development of an injector durability stand for evaluation of wear rates in fuel injectors. The first two of these areas have resulted in valuable information about the limitations of lubricity and viscosity additives that are presently available in terms of their impact on the viscosity of DME and on wear rates on injector hardware. The third area, that of development of an injector durability test stand, has not resulted in a functioning experiment. Some information is provided in this report to identify the remaining tasks that need to be performed to make the injector stand operational.

The lubricity apparatus has been constructed by adding a high pressure cell to an existing Cameron-Plint reciprocating wear machine that generates the reciprocating wear of a test specimen (pin) against another surface (cylinder). The pin and cylinder are constructed of the same materials used by Caterpillar in the fabrication of the Hydraulic Electronic Unit Injectors (HEUI) that are used in the Navistar V-8 turbodiesel engine in the DME Shuttle Bus project.

The injector durability stand was originally going to be fabricated at Penn State with input from Navistar and Caterpillar, both of which have provided support for the DME research at Penn State. Then, Caterpillar expressed confidence that a HEUI Endurance Stand could be donated for the project to eliminate the need to build a complicated stand at Penn State. However, the Caterpillar donation fell through and we began the process of building an injector stand at Penn State using students who were pursuing their senior design projects and hardware from the DME Shuttle Bus.

The key observations from the work are that when blended at 25 wt.% in either diesel fuel or Biodiesel fuel, DME requires more than 5 wt.% additive of all viscosity and lubricity additives tested here to even approach the lower limit of the ASTM diesel fuel viscosity requirement. To treat neat DME sufficiently to make DME comply with the ASTM diesel fuel viscosity requirement would require a viscosity additive with 10^{45} cSt viscosity, which is not possible with current additive technologies.

EXPERIMENTAL

Introduction

This project is driven by the desire to utilize dimethyl ether as an ultra-clean transportation fuels. Dimethyl ether (DME) can be a replacement diesel fuel that lowers emissions significantly, if it's low lubricity and low viscosity can be overcome. There are two methods for utilizing DME: design injection systems that can tolerate the low lubricity and low viscosity of DME; or develop fuel formulations (through blending or additives) that give physical properties to DME mixtures that fall within conventional diesel fuel ranges. Following the latter approach, we have been examining the co-firing of the engine on diesel fuel and dimethyl ether, using the diesel fuel as a lubricating agent to protect the fuel pump and fuel injection system from excessive wear. Dimethyl ether has no natural lubricity, making it antagonistic to fuel system components.

The interest in operating diesel engines on DME arose initially from a collaboration between Penn State and Air Products and Chemicals to develop a campus shuttle bus that could operate on DME. That project, which is also supported by the Pennsylvania Department of Environmental Protection and the National Energy Technology Laboratory (agreement # DE-FG29-99FT40161), has focused on blending DME with sufficient diesel fuel to provide an acceptable mixture viscosity and lubricity to be compatible with existing diesel engine technology.

Due to the low viscosity of DME (on the order of 0.2 cSt at 40°C [1]), the blend ratio that the shuttle bus project was limited to is 25 wt.%, a finding that has come out of the other NETL-sponsored project. Figure 1 shows the blend response of the mixture viscosity to variations in DME content.

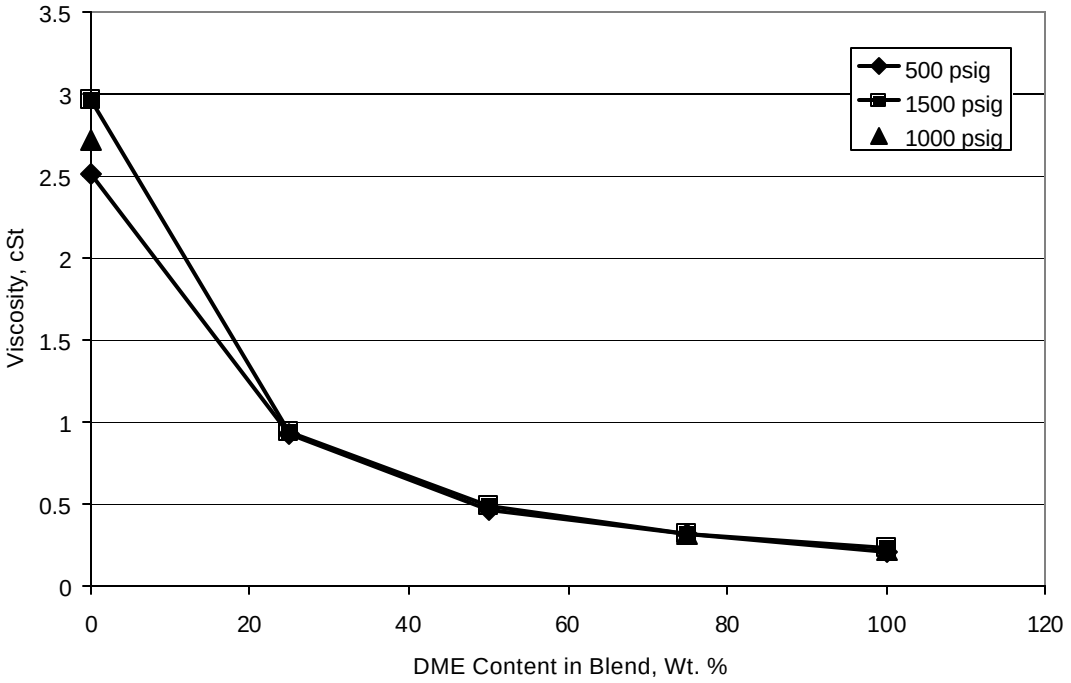

Figure 1. Viscosity – DME Content Relationship at Different Pressures @100 F

As Figure 1 shows, at 25 wt.% DME the viscosity drops to roughly 1.39 cSt, which is the lower limit of the ASTM specification for diesel fuel viscosity. To increase the allowable DME without exposing the injectors to excessive wear and early failure, both the lubricity and the viscosity of the fuel blend must be kept within the ASTM specifications. To that end and to raise the allowable DME content in the mixture, the present work focuses in parallel on selection and development of additives to improve lubricity and viscosity of DME fuel blends.

In our laboratory engine, we have demonstrated effective operation on the 25 wt.% DME blended fuel. In the field, we successfully demonstrated the operation of a campus shuttle bus on blends of DME in diesel up to 25 wt.% DME [1]. Through collaboration with the Tribology Laboratory in Penn State's Chemical Engineering Department, we are characterizing the viscosity, compressibility and miscibility of blends of DME, diesel fuel and the additives under pressures and temperatures relevant to the fuel injection system. These tests are using a high pressure viscometer adapted to these specific experiments. This instrument, combined with a high pressure cell for lubricity studies and an injector durability stand to demonstrate injector time-to-failure, provides us with the ability to determine if additives can be used to increase DME content in the blended fuel while not sacrificing injector lifetime.

At present, we have completed an initial screening of the impact on the viscosity of DME of various lubricity additives and high lubricity fuels. This work has resulted in a manuscript that has appeared in *Energy & Fuels* [2]. In addition, we have examined a range of additives in a modified Cameron-Plint reciprocating wear test apparatus to investigate the lubricity of DME blends with diesel fuel and lubricity and viscosity improvers. After failing to acquire a donation of an injector durability test stand, we are also working to develop our own inexpensive injector durability stand using students from senior design classes and hardware from the now completed DME Shuttle Bus project.

Caterpillar (manufacturer of the HEUI fuel injectors on the Navistar T444E turbodiesel engine) had agreed to participate in this project on injector durability and they have already provided 6 sets of HEUI injectors (8 injectors per set, total retail value of over $24,000) for this project. One set was installed in the DME Shuttle Bus to provide some field data on wear rates using DME diesel blends. The rest of the injectors will be used in the injector durability stand. Unfortunately, due to difficult financial time, Caterpillar was not able to follow through on the donation of a HEUI Endurance Stand for the injector durability studies. However, Caterpillar did complete a post mortem analysis of the fuel injectors that were operated for three months with DME blended fuel on the DME Shuttle Bus. Caterpillar found that the injectors had suffered some damage to their internal components, but could not explain how. This provides evidence that DME operation can lead to unexpected injector behavior, and confirms the need for the present project.

Background. The need to reach ever tightening NOx and particulate emissions standards has placed a tremendous amount of pressure on fuel, lubricant, engine and vehicle manufacturers. However, in the 1990's studies of direct injection diesel engines fueled by dimethyl ether (DME) demonstrated particulate emissions below the ULEV standard and NO_x emissions that approach or achieve ULEV levels, *without exhaust aftertreatment* [3,4]. As a consequence, DME is gaining increasing interest for use in compression ignition (CI) engines as a replacement diesel fuel. Until those tests, DME had not been considered as a primary replacement fuel. Previously,

DME had been considered as a methanol ignition improver for methanol powered vehicles [5,6,7,8]. At present, the predominant use for DME is as an environmentally benign aerosol propellant, since DME is non-toxic and is easily degraded in the troposphere [9]. Recent work on DME has focused on its use in advanced technology, direct-injection (DI) engines as a neat fuel [10,11,12,13,14]. Due to the presence of an oxygen atom in DME's molecular structure, the absence of a carbon-carbon bond and its high cetane number, the DME-fueled engine appears to circumvent the traditional tradeoff between oxides of nitrogen (NOx) and particulates that plagues the CI engine running on diesel fuel. The high cetane number of DME also helps in reducing combustion noise, which is another drawback of the diesel fuel fired CI engine [3,4,15,16,17,18,19]

DME is the simplest ether compound (chemical formula C_2H_6O). Some physical and chemical characteristics of DME are given in Table 1. At standard temperature and pressure it is a gas, but can be liquefied under a moderate pressure. This makes DME quite similar to propane and liquefied petroleum gas for handling purposes. DME was first used as an aerosol propellant because of its environmentally benign characteristics. It is not harmful to the ozone layer , unlike the CFCs that it replaced. DuPont Fluorochemicals provides a technical information bulletin [20] that gives a good overview of the physical and chemical properties of DME.

Table 1: Physical and Chemical Properties of DME [20]

Chemical formula	H_3C-O-CH_3
Molecular weight	46.07
Oxygen content by mass	34.8 %
CAS Registry number	115-10-6
Boiling point @ 1 atmosphere	-24.825 °C
Critical temperature	126.85 °C
Critical pressure	5370 kPa
Liquid density @ 25 °C	656.62 kg/m3
Vapor pressure @ 20 °C	516.76 kPa
Flammability limits in air by volume %	3.4 – 18

A high cetane number makes DME an attractive fuel for compression ignition (CI) engines. However, DME has significantly different physical properties than diesel fuel including a low critical point, low viscosity, negligible lubricity and a high vapor pressure. As DME has a high vapor pressure, the fuel system needs to be pressurized to maintain DME in a liquid state. Moreover, the fuel system has to be modified considering the chemical properties of DME, such as its incompatibility with many elastomers. In the present work, DME has been blended into diesel fuel to obtain a fuel mixture that retains the desirable physical properties of diesel fuel but includes the cleaner burning capability of DME. The miscibility and viscosity of blends of DME and diesel fuel were characterized using pressurized, optically accessible instrumentation. These physical property measurements are part of a comprehensive study of the operation of a turbodiesel engine on DME-diesel blends which led to a field demonstration of this fueling strategy [21,22,23]. In the culmination of the demonstration, a campus shuttle bus was operated on blends of DME and diesel fuel on a shuttle route at the University Park campus of the

Pennsylvania State University in the first operation of an in-service transit vehicle on DME anywhere in the world [23].

Diesel fuel injection systems are designed for diesel fuel, which has a kinematic viscosity an order of magnitude higher than that of pure DME, as evidenced by the ASTM standards for diesel fuel properties [24]. In this paper, the viscosity of DME in blends with various fuels and additives is examined to determine whether the mixture viscosity can be improved via blending or additization. These viscosity measurements are among the first reported for DME under elevated pressures and are the first reported for blends in diesel fuel.

Recent work by Sivebaek et al. [25] also considered the viscosity of DME, in particular with addition of lubricity and viscosity enhancing additives. They developed a volatile fuel viscometer (VFVM) that was designed to handle DME, neat or additized. They measured kinematic and dynamic viscosities of pure DME of 0.185 cSt and 0.122 cP at 25 °C, which as will be shown, compares well with the present study. Their measurements were performed at 5 bar pressure, roughly 75 psi. They concluded that additized DME cannot reach the same viscosity and lubricity as diesel fuel. They suggest that rather than using additives to allow fuel systems to tolerate DME, the solution is to design fuel injection hardware to handle pure DME.

McCandless and co-workers have developed models for the properties of DME and have developed fuel injection systems to accommodate neat DME (or more specifically, DME with 1% of a castor oil additive) [13,26]. Their approach has been to develop systems with less of the sliding wear that leads to pump and injector failures that were observed in earlier work on DME.

In contrast, the work presented here involves accommodating DME within existing, commercial fuel injection systems. Thus, there is a need to determine how to improve the viscosity of DME fuel blends, while keeping the DME content as high as possible to capture the emissions benefits of DME. To that end, the viscosity measurements of DME blended with various fuels and with various lubricity enhancing additives is intended to assess whether the viscosity of DME can be increased with only modest treat rates of other substances. The work presented here is the product of a joint effort by the Penn State Energy Institute and Multi-discipline Tribology Group, which have collaborated on studies of several alternative fuels including biodiesel fuels [27] and oxygenated fuels [28]. Significant improvements in friction and wear were demonstrated by vapor-phase oxidation of biodiesel fuels [29].

High Pressure Viscometry and Miscibility Studies

Two different high pressure cells were adapted for studying the miscibility and viscosity of blends of DME and diesel fuel. One permitted the fuel mixtures to be held at pressures up to 200 psi to examine miscibility by visual inspection of blends over extended periods of time. The fuels were deemed to be miscible if no evidence of phase separation was observed. The other instrument is a high pressure viscometer consisting of a capillary tube held within a pressurized chamber suitable for measurements at pressures up to 3500 psi.

Miscibility Measurements. Qualitative studies of the miscibility of blends of DME and a federal low sulfur (300 ppm) “emissions certification” diesel fuel (Specified Fuels “ECD LS”) were performed under pressures above 90 psi. Blends from 25 wt.% DME up to 75 wt.% DME

in diesel fuel were examined. Diesel fuel was gravity fed into an optically accessible pressure chamber, while DME was delivered from a cylinder of liquefied DME through an opening in the bottom of the pressure chamber. Pressures in the chamber were raised by feeding nitrogen above the fuel mixture to attain 90 psi or greater in the chamber.

Viscosity Measurements. Quantitative measurements of the viscosity of blends of DME in the federal low sulfur fuel were obtained using a high pressure viscometer, using capillary tubes that provided optimal measurement accuracy depending on the viscosity of the fuel mixture. The high pressure viscometer apparatus used for this work was designed and built at The Pennsylvania State University in 1962-63. This equipment was modified to allow for charging of pressurized liquid samples, as is necessary when dealing with compressed liquids. Johnson [30]in his Master's thesis, gives a detailed description of the design and use of the apparatus. The equipment, very simple in design, nevertheless is extremely accurate in viscosity measurement up to a pressure of 10000 psig. The viscometer instrumentation consists of a pressure intensifying system, a pressure measurement system, a constant temperature bath and the viscometer pressure vessel.

Fig. 2 shows a sketch of the high pressure viscometer apparatus. Pressurized helium produces the high pressure required for this equipment. Pressures up to 2000 psig can be attained by simply connecting a commercial helium gas cylinder to the system. For higher pressures, the air operated pressure intensifying pump is used. This system consists of an AMINCO dehydrogenation bomb with a volumetric capacity of 4.5 liter. This bomb is filled with helium from the gas bottle at the available pressure. This is further compressed by pumping oil into the bomb. A SAE30 oil was used in this case. For higher pressures, however, a SAE50 oil is recommended. The oil is pumped by an air driven pump (Teledyne Sprague Engineering Model # S-216-J-150). The 150 in the model number indicates the factor by which the pressure of oil can be raised as compared to the pressure of the supplied driver air. High pressure gauges are used to measure the pressure in the system. These gauges have a maximum readability of 5000 and 10000 psig and have a rated accuracy of 0.5% of full scale. For the present study, the gauge with a capacity of 5000 psig was used for its higher resolution. For the present study, the viscometer housing was kept at a constant temperature of 100°F (38°C) in a water bath.

Prior to beginning the viscosity measurement, the sample is prepared in the sample cylinder and maintained at a pressure of about 500 psig. The sample cylinder is then kept in the water bath overnight to ensure thermal equilibrium between the sample and the water bath. The AMINCO hydrogenation bomb is charged to the required pressure by operating the pressurizing equipment. The viscometer capillary is assembled in the pressure vessel and is brought up to the operating pressures. The following steps are then taken to charge the viscometer capillary with the fluid and measure its viscosity. Samples of fuels or blends are prepared in a sample cylinder. The sample cylinder is connected to the viscometer housing, pressure is allowed to equilibrate between the sample cylinder and the viscometer housing, and sample is introduced into the capillary tube. The level of the sample is observed through the glass windows on the viscometer housing. Then, the viscometer is allowed to reach thermal equilibrium between the capillary, housing and sample.

The measurement of viscosity is performed by measuring the time required to drain fluid from the capillary, as the meniscus in the capillary falls past two etched lines on the capillary. Fig. 3 shows the locations of the etchings and the configuration of the capillary tube. The time is measured with a resolution of 0.01 seconds. The measured efflux time along with the characteristic distance are the only two observations required of the viscosity test. The characteristic distance is the distance between the liquid level at the bottom of the viscometer housing and the bottommost etched line on the capillary. This distance is measured by a cathetometer with a resolution of 0.005 cm.

The procedure followed for calibration of the viscometer is the same as that followed for viscosity measurement. The calibration is performed by allowing a liquid with a known viscosity to drain from the capillary. A series of runs are performed by varying the characteristic height. For every run, the characteristic height and drainage time are recorded. A viscometer constant is calculated via Equation 1:

$$\text{viscometer constant (s/cSt)} = \text{drainage time (s)} / \text{viscosity of calibration liquid (cSt)} \quad (1)$$

Fuel and Additive Samples. The DME was obtained from DuPont Fluorochemicals and is highly purified, having less than 20 ppm water content. The diesel fuel is a federal low sulfur fuel, emissions certification diesel fuel from Specified Fuels (ECD-LS). The biodiesel fuel was obtained from World Energy as 100% biodiesel (B100 “Envirodiesel’). Lubricity additives were obtained from Lubrizol Corporation (539N) and Ethyl Petroleum Additives, Inc. (“HiTEC Performance Additives” 4140 and 580, referred to here as H4140 and H580). The soybean oil was provided by Agricultural Commodities, Inc. and was produced from soybeans through a heated extrusion and press process. The viscosity of these fuels and additives are presented in Table 2, along with some other physical and chemical property information.

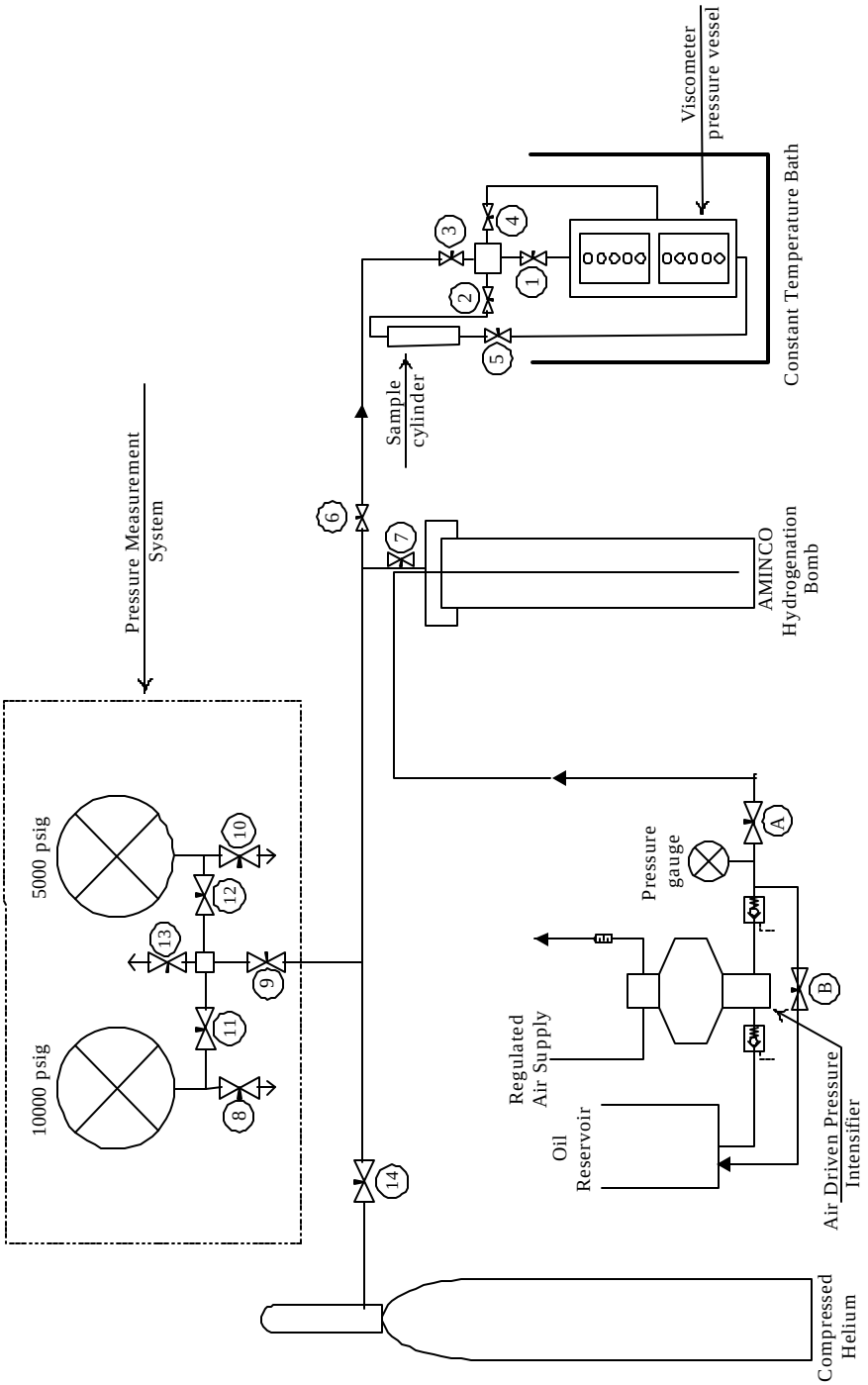

Fig. 2. High pressure viscometer configuration

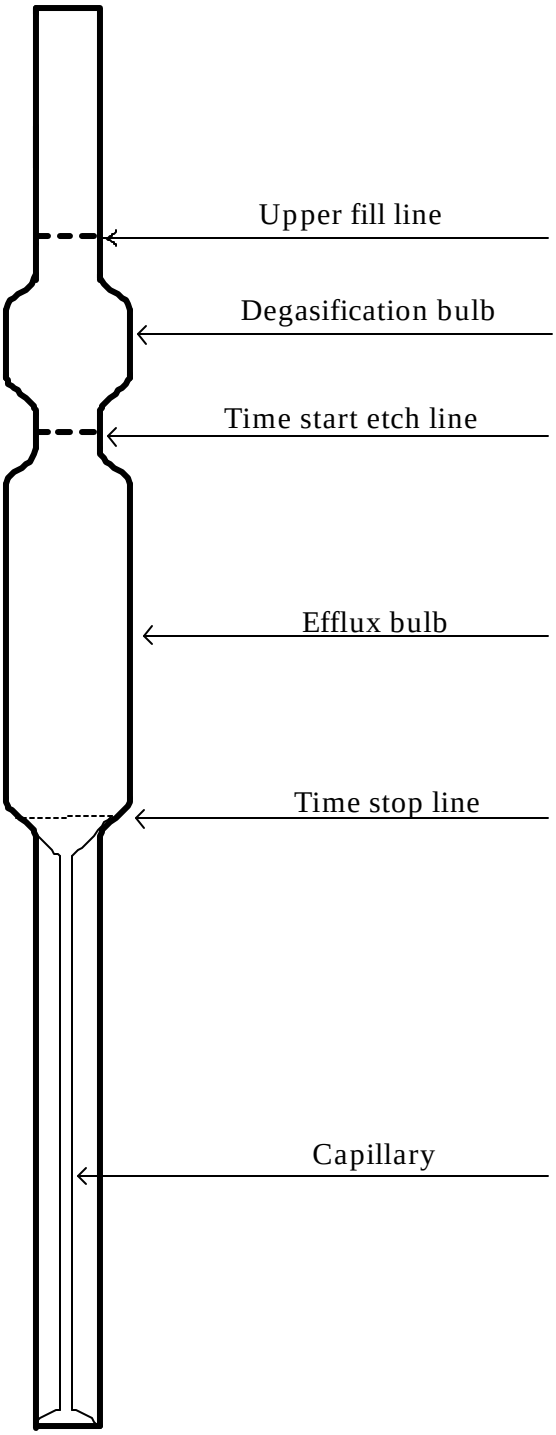

Fig. 3. Capillary viscometer configuration.

Table 1. Viscosity of fuels and additives

	ASTM Method	ASTM Spec.	Base Diesel	DME (75 psi)	Biodiesel (B100)	Soybean Oil	Ethyl H4140	Ethyl H580	Lubrizol 539N
Viscosity, 40°C, cSt	D 445 [31]	1.39-4.20	2.5	0.185	4.1	31.3	17	110	31.4 (@25°C)
Viscosity, 100°C, cSt			1.1		1.7	7.6			

Novel Viscosity Test Apparatus

This section details the design and operation of a new pressurizable capillary viscometer. A closed system is necessary in order to allow operation with materials that are a gas at standard temperature and pressure. No capillary viscometer is currently available to conduct measurements of fluids such as DME, ergo, one was constructed for this study. The basic design is borrowed from a traditional glass capillary viscometer, which is open at one end to the atmosphere. The ASTM approved operating instructions can be found in ASTM D445. Figure 4 shows a drawing of the instrument including all critical measurements:

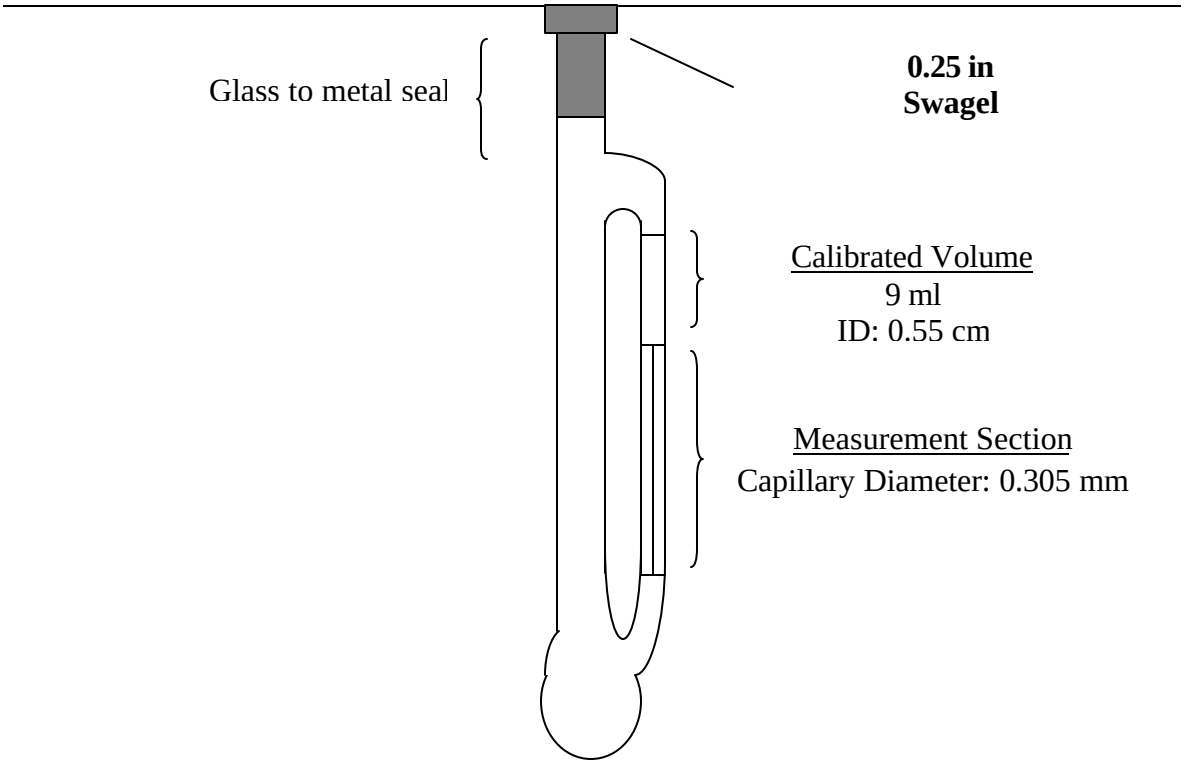

Fig. 4: Drawing of the pressurizable glass capillary viscometer

In order to create a solid, pressure safe seal, a glass to metal bond was necessary. The type chosen for this work was purchased from The Kurt J. Lesker Company and is a direct 3/8" OD stainless steel to Pyrex connection. Other manufacturers grade the glass types close to the transition point to match the thermal expansion properties of the glass and metal, reducing cracking potential. This trademarked seal has no such problems. Other seal types utilize a glass to copper seal. A copper seal was tried, but the corrosive nature of copper led to system depressurization. Pressure testing of the instrument revealed that the seal, and glass walls, were capable of holding at least 800 psi nitrogen for an indefinite period of time.

In order to fill the unit with dimethyl ether (DME), the entire instrument was first cooled in a dry ice/acetone bath after recording the initial weight. A small sample cylinder containing DME was attached to a ring stand and the viscometer attached directly below the cylinder's exit. A 1/16" stainless steel tube connected to the cylinder outlet was threaded down the main (wide) section of the viscometer to the bulb at the base. DME was added to the viscometer until the lower bulb was filled to capacity. There is a finite range of acceptable fluid volumes for this instrument. There must be a clear pathway between the capillary exit and the viscometer body to maintain a constant fluid head, and to make one measurement or run, it is necessary that there is enough fuel present to occupy the entire calibration volume. After filling the viscometer, the tubing was then quickly removed and the top caped off. The viscometer was then warmed to room temperature, dried, and weighed again to determine the amount of dimethyl ether added. If a blend was the goal, diesel was weighed into the viscometer and a pre-calculated volume of dimethyl ether was added via trial and error. The addition of additives required multiple weightings and calculations prior to DME addition.

All viscosity measurements were performed at 25 and 40^{o}C in a 30 gallon constant temperature water bath complete with stirring motor, heating, cooling and control elements. Temperature was controlled via the thermostat, but was also monitored by an independent ASTM kin-visc calibrated thermometer accurate to +/- 0.005^{o}C. The deionized water (used so no buildup occurred on the glass) was allowed to equilibrate the temperature of the viscometer for at least 30 min.

A tilting metal arm apparatus was used to hold the viscometer in the bath. This configuration was conducive to re-filling the calibration volume without having to remove the instrument from the water bath. To fill the viscometer, the instrument was tipped so liquid ran from the lower bulb to the upper calibration region. To make a measurement, the unit was repositioned and as the liquid level passed the top mark, a timer was started. When the fluid meniscus reached the lower mark, the timer was stopped. This process was repeated 10 times for each fluid tested and an average taken. Knowing a few additional simple parameters, the average time was used to directly calculate the viscosity.
The governing equation for capillary viscometers stems from the Bernoulli Equation shown in Eq. **2**:

$$u = \frac{10^6 pgD^4 Ht}{128VL} - \frac{E}{t^2} \qquad \textbf{(2)}$$

Where ν is the kinematic viscosity, g is the acceleration due to gravity, D is the diameter of the capillary, L is the length of the capillary, H is the average distance between upper and lower menisci, V is the timed calibration fluid volume, E is kinetic energy correction factor and t is the flow time. As long as the viscometer is designed so a minimum flow time is exceeded, the kinetic energy term, E/t^2, becomes insignificant. It is also possible to simplify the equation by combining all the constants into one term, called C, as shown in Eq. **3**:

$$u = Ct \qquad \textbf{(3)}$$

Since C is only dependent on viscometer properties, one can use a fluid of well-known viscosity to "calibrate" the viscometer and experimentally derive C. Once this constant is established, it can be used with fluids of unknown viscosity, as long as the minimum flow time is reached. The kinetic energy term is investigated in more detail in the Results and Discussion section.

After all measurements at two temperatures are complete, the viscometer is emptied by slowly unscrewing the Swagelock® cap. The inside and cap are fully washed with tetrahydrofuran, naphtha and acetone to remove any residue. Once drying is complete the unit is prepared for the next fluid.

Cameron-Plint Wear Test Apparatus

The goal of modifying and using this instrument was to mimic the operation of a fuel injector. Before the modifications are discussed, a brief summary of the initial geometry and performance capabilities is presented.

The traditional Cameron-Plint wear tester is designed to study friction and wear in dry or lubricated tests at room or elevated temperatures. The test operates in a reciprocating motion and load can be varied. Several possible contact geometries, including pin on disk and ring on liner, can be adapted. The Penn State unit is a model TE77 capable of recording friction and temperature. There is a load arm with variable weight configurations and a motor that drives the test operating in the range of 0-50 Hz. The unit has the ability to operate from 0-600^{o}C with 2-250 N of applied load.

The system was modified to better match the operation of a fuel injector. A new head configuration was designed to mimic actual operation as closely as possible. The motor shaft was used to drive a plunger and coupler in and out of a stainless steel pressurizable housing containing a matching outer barrel and the fuel of choice. Schematic diagrams of the head assembly are shown in Figure 5.

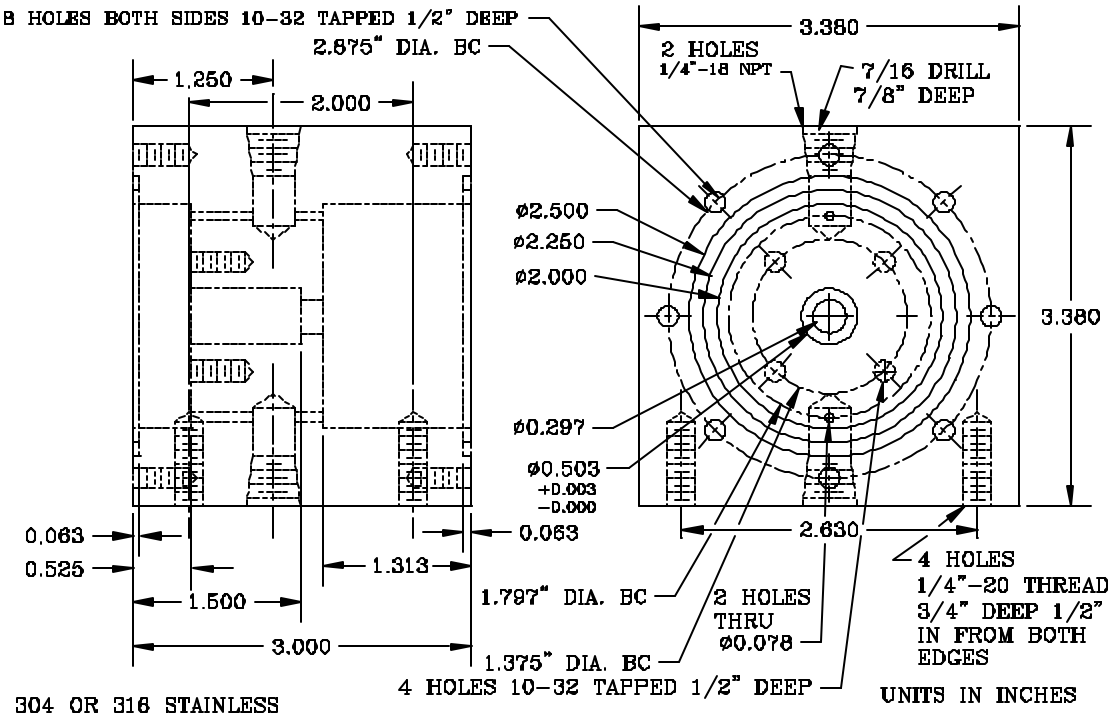

Figure 5: Cameron-Plint head assembly

The housing contains several components. There is a stationary body consisting of two stainless steel sides 3.5" tall by 0.525" thick and a top welded together and fixed via setting screws to a large metal base. The left and right walls are removable, the right being solid and assembled via screws. The left wall has an opening for the motor shaft and several o-ring grooves. Static Kalrez® o-ring face seals are used on both walls. The internal compartment is solid with two exceptions; first, there is a cylindrical opening with a holding lip in the center to house the outer barrel. The barrel is held in place by two 1.375" round plates, one in front the other in back, that screw into the solid core. There is an opening in the bottom of the chamber for venting, one in the top for filling and pressure measurement, and a small hole drilled inside the chamber parallel to the base plate to facilitate fluid motion and mixing.

The greatest challenge in designing this system was the shaft seal/coupling. The pin component, the mate to the outer barrel, was first placed into a holder. The holder consisted of a 0.525" thick disk, with a wedge missing, and a hole drilled in the center for pin insertion. A setscrew was tightened to ensure the pin remained in the holder. Beyond the disk, a solid stainless steel shaft, the same diameter as the motor shaft, extended through an opening in the left wall.

Maintaining a proper seal was extremely difficult around the moving shaft. The final design utilized a Kalrez® o-ring (the o-ring sealing requirements motivated a study of elastomer compatibility, the results from which can be found in the doctoral dissertation of K. Wain [32]) on the inside of the housing, and a Teflon o-ring on the outside of the housing. Both o-rings were SAE-206 and were set into properly machined grooves to maximize system stability. In

order to ensure the o-rings stayed in place, smooth circular backup plates were screwed into the left wall to finger tightness. Krytox® fluorinated grease was used on the o-rings to reduce friction and wear. The system alignment was automatic upon assembly, but care was always taken to ensure pristine condition of test specimens. The final piece assembled was a coupler for the motor shaft-pin holder joint. This metal cylinder had a wedge missing along the length and four screws to allow proper tightening of the seal.

Test Specimens. The success of this test was dependent on the ability of a machinist to properly replicate the injector plunger and barrel (outer cylinder). Injector tolerances are extremely precise and tight in order to maximize performance and efficiency. The curvature in the specimens also adds to the machining difficulty. All dimensions were measured from an actual injector or as stated from the manufacturer.

The outer cylinder has a bore inside diameter (ID) of 0.2360 +0.0001/-0.0000 inches and an outside diameter (OD) of 0.500 +0.000/-0.001 inches. The surface finish (Ra) is better than 10 micro-inches on the inside surface. The material of construction is 52100 stainless steel with a Rockwell Hardness of 62. The length of the specimen is 1.000 +/- 0.005 inches.

The matching pin is also 52100 steel with a Rockwell Hardness of 62. The length of the specimen is 1.575 +/- 0.005 inches. This solid pin has an OD of 0.2359 +0.0000/-0.0001 inches. Combined, these dimensions mimic an actual injector yielding a clearance of 0.0001" minimum and 0.0003" maximum, or better than 6 microns. The shop chosen to make these components was Dixon Tool and Dye Inc. in Tyrone, PA.

Fuel Blending. For all wear testing, as well as elastomer experiments, it was necessary to create fuel blends of dimethyl ether and diesel fuel, with and without additives. The steps to creating fuel blends are straight forward but involved, and are described in detail in this section.
The fuel vessel is a stainless steel cylinder with an internal volume of 300 ml. Both ends of the vessel were fitted with Kalrez® valves, along with a pressure gauge at the top. Blends were first calculated by assuming a final volume and calculating the weight of each fuel component needed. Diesel fuel was added first, using a syringe, and the vessel was weighed on a balance to ensure the correct volume addition. Dimethyl ether was added from a pressure cylinder with a helium over-pressure of 200 psi through the lower connection in the fuel cylinder. Quick opening and closing of the valve was used to allow only small DME additions. After each addition, the vessel was weighed to determine if further additions were necessary. If additives were included, they were first blended into the diesel fuel in the initial stage. By adding DME from the bottom of the vessel, it was assumed turbulent mixing occurred. This fuel mixture was then transported to where testing took place.

System Integration and Operating Procedure. The section details the operation of the modified Cameron-Plint. Included are all test methods and conditions. For reference, the system, excluding the detailed head assembly, is diagramed in Figure 5.

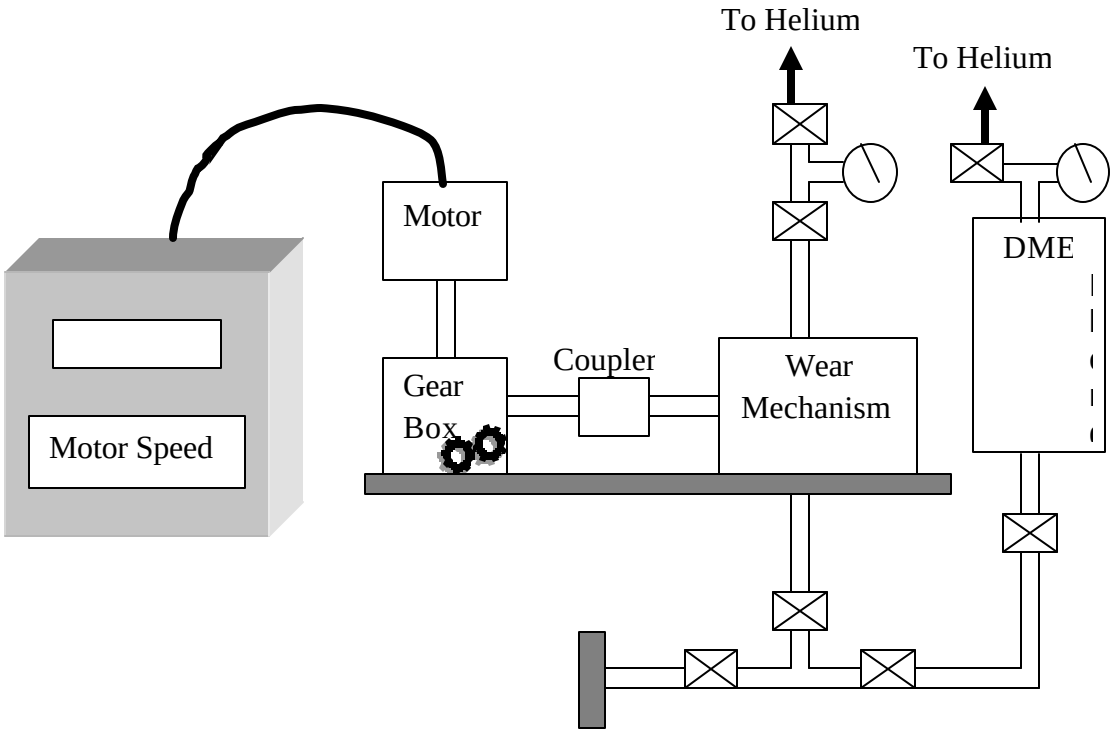

Fig. 6: Modified Cameron-Plint wear tester configuration

Once the head is assembled and alignment is confirmed, the housing is pressure tested. Pure helium is added to the chamber at 150 psi. The head is isolated with a series of Kalrez® valves while system integrity is checked. The motor shaft is manually turned several times to ensure a dynamic seal is also present. Once the system is deemed acceptable, the helium pressure is lowered to ~60 psi.

The next step is to add the fuel blend of interest to the chamber. This is accomplished by using helium as a driving force at the upper connection of the fuel cylinder. The valve train is opened so fuel enters from the bottom of the wear mechanism. A sight glass located just above the wear mechanism chamber allows visual confirmation of the fuel level. The 60 psi helium head is established in order to ensure no vaporization of DME during the filling process. Once the fuel has reached the appropriate level, additional helium is added until the total system pressure is 150 psi. This pressure is maintained throughout testing.

Before beginning the test, the system seals are checked again. Finally, the power is switched on and the motor is started. The speed is slowly ramped up to 10 Hz. This speed is maintained for 15 min, and is used as a safety step in case of sudden depressurization. After the 15 min buffer, the motor speed is increased to 40 Hz and maintained for 3 hours.

After the test is complete, the motor speed is slowly reduced to zero. The fuel is then removed via the lower drain line valve train and collected for future analysis. The unit is disassembled starting with the shaft coupling. Both the pin and barrel are removed and wrapped in tissue. The unit is then thoroughly cleaned with tetrahydrofuran and acetone. All o-rings are removed and

saved for further analysis. Wear specimens are cleaned via 3 min sonication steps in tetrahydrofuran, naphtha and acetone.

The dimensions of the components allowed for reuse in some cases. The total travel distance of the pin in the barrel is 4 mm. The length of the barrel is 1 in, significantly longer than the travel distance. In most cases, the barrel was reused by flipping the specimen to the un-worn edge and inserting a new pin. Since the screws of the pin holder scuffed the non-test end of the pin, a new pin specimen was required for each test.

Profilometry. Initially, weight loss was used to study the wear rate. Due to the low loss of mass, to quantify the wear on the pin and cylinder an image mapping technique was necessary. To use this technique, the outer barrel was first cut in half length-wise to expose in interior for mapping. All specimens were engraved with a unique identifier for accounting purposes.

The specific instrument used was a MicroXAM™ Surface Mapping Microscope (ADE Phase Shift; Tucson, AZ). This device probes a surface by generating a horizontal plane of light that moves in the z-direction. Successive interaction between the light plane and the sample generate a unique reflectance signal that in turn allows the creation of a surface map. The instrument has a total z-direction motion of 100 μm and lenses from 5x to 100x magnification. A DOS based software package interprets the signals and forms a complete image. Maps can be further enhanced using smoothing and other feature altering tools.

RESULTS AND DISCUSSION

This section of this report consists of sub-sections on each of the major activities (tasks) under the project.

- Task 1. Wear Rate and Lubricity Measurements of DME-Diesel Fuel Blends
- Task 2. Injector Durability Studies

Task 1. Wear Rate and Lubricity Measurements of DME-Diesel Fuel Blends

Viscosity Measurements of Lubricity Improvers

Miscibility Measurements. The DME was observed to rapidly mix uniformly with the diesel fuel at all blend ratios. Over time, a blend that was initially not well mixed would become uniform, but injection of the DME from below the pool of diesel fuel was a particularly effective means of rapidly obtaining a uniform mixture. The biodiesel and soybean oil samples and the lubricity additives mixed uniformly with DME and remained mixed over time, at the concentrations examined here.

Viscosity Measurements. Observations of the viscosity of the blends of DME and diesel fuel are summarized in Fig. 7. Measurements were obtained over a range of pressures with the viscometer housing immersed in a constant temperature bath at 100°F (38°C). Results obtained at three different levels of chamber pressure are plotted in Fig. 8 to show the impact of DME content on viscosity.

These two figures show that the viscosity of diesel fuel decreases rapidly at low levels of DME addition. For instance at 25 wt.% DME addition, viscosity falls by more than a factor of 2, from the more than 2.5 cSt value of the neat diesel fuel to roughly 1 cSt. This non-linear blending response demonstrates that even modest addition of DME to diesel fuel brings the fuel blend below the ASTM diesel viscosity specification of 1.39-4.20 cSt at 40°C [24]. This result is predicted using the ASTM oil blending calculations method D 341 [33]. According to this method, oils blend in a logarithmic fashion, allowing a small amount of a low viscosity component to have a large effect on blend viscosity. Predicted blend viscosities, shown in Fig. 8, match the experimentally observed trends.

These viscosity measurements are among the first reported for DME under elevated pressures and are the first reported for blends in diesel fuel. Sivebaek et al. [25] considered the viscosity of DME, in particular with addition of lubricity and viscosity enhancing additives, using a volatile fuel viscometer (VFVM). They measured kinematic and dynamic viscosities of pure DME of 0.185 cSt and 0.122 cP at 25 °C, respectively. Their measurements were performed at 5 bar pressure, roughly 75 psi. In the present study, no DME blends were examined at a pressure below 500 psi, but at 500 psi pressure the viscosity of neat DME was found to be 0.21 cSt. Extrapolating data for neat DME from the present study at 500 psi to a pressure of 75 psi yields an estimate of 0.2 cSt, which is in reasonable agreement with the value of 0.185 cSt obtained using the VFVM. In general, the viscosity-pressure relationship is weak. Temperature and molecular weight have far more significant impacts.

Sivebaek et al. concluded that additized DME cannot reach the same viscosity and lubricity as diesel fuel [25]. In separate work, Sivebaek and Sorenson [34] showed that at 900 ppm addition of Lubrizol 539N to DME, a wear scar diameter equivalent to diesel fuel could be obtained. However, as pointed out in Sivebaek et al. [25], Nielsen and Sorenson [35] found that DME with 900 ppm of Lubrizol 539N addition does not prevent premature wear in injection pumps. Sivebaek et al. [25] suggest that rather than using additives to allow fuel systems to tolerate DME, the solution is to design the pumps so that they can handle pure DME. From these observations by Sorenson and co-workers, it appears that while the lubricity of DME can be increased with additives, viscosity must also be increased to prevent premature wear of injection systems. To examine this issue of whether the viscosity of DME can be increased with additives, the viscosity of DME was measured with vegetable oil fuels from 1000 ppm to 50% addition and with three lubricity additives from 1000 ppm to 1% addition. The vegetable oil fuels were also added at levels up to 20 wt.% (soybean oil) and 50 wt.% (biodiesel), to look for a threshold of additive addition that yielded a mixture viscosity approaching the lower limit of the ASTM diesel fuel standard, 1.39 cSt [24].

Fig. 9 and 10 show the results of blending DME with biodiesel and soybean oil, respectively. The viscosity of the mixtures of vegetable oils and DME are compared with neat DME, 25 wt.% DME in Diesel fuel and 50 wt.% DME in diesel fuel. The data show that despite their elevated viscosity relative to diesel fuel, the soybean oil and its methyl ester (biodiesel) provide only a modest improvement in mixture viscosity when compared on a weight addition basis. At 50 wt.% addition to DME, biodiesel yields a 22% higher viscosity than diesel fuel. At 20 wt.% addition, both biodiesel and soybean oil provide roughly a 16% higher viscosity than diesel fuel. Although soybean oil has a viscosity more than 10 times higher than diesel fuel, only small changes in viscosity were observed. ASTM blending methods, although designed only for petroleum oil mixtures, predict this trend as well. In fact, mixture calculations show that roughly 5 wt. % DME in a 50 wt. % soybean-50 wt. % diesel mixture cause the viscosity to drop below the 1.39 cSt ASTM limit. The ultra low viscosity of DME is the dominating factor in blend viscosities.

Figures 11-13 show the impact on viscosity of addition of lubricity agents to DME. As in Figures 9 and 10, comparison is shown with neat DME, 25 wt.% DME in diesel fuel and 50 wt.% DME in diesel fuel. The additives were not examined at the elevated levels (>1 wt.% addition) that the vegetable oils were because they do not have the availability to constitute blending agents, and could only be used at modest concentrations. However, it was valid to test if the high viscosity of these compounds, over 100 cSt for the Ethyl H580 additive, boosted the viscosity of DME at low levels. As shown in Fig. 12, the H580 additive provided only a 5% increase in viscosity at 1 wt.% addition. Similarly weak results were obtained with the Ethyl H4140 and Lubrizol 539N additives.

Unlike diesel fuel molecules, DME does not contain any long chain components, limiting additive-fuel interaction. Typically the C_{12}-C_{24} chains of diesel will entangle with viscosity improving molecules, increasing the mixture viscosity. DME also allows little or no hydrogen bonding to occur. The solution to proper lubrication of injection system components may lie not in the ability to increase the viscosity of DME up to ATSM standards, but in the ability of

additives to form a protective surface film on the wearing metal components. Typically these types of additives are polar in nature and potentially contain aromatic rings and/or double bonds to enhance molecular interactions. This increases the potential for physical or chemical adsorption to metal surfaces. In viscosity improvers, polymer molecules "swell" in the presence of fuel. The volume of the swollen mixture dictates the degree of viscosity improvement. A protective surface film would not be subject to this swelling mechanism and may therefore improve lubricity via another method.

Thus, it is clear from the present work and the previous studies by Sivebaek et al. that lubricity agents do not provide effective means of boosting the viscosity of DME at treat rates that are relevant for additives. However, plant oil-derived fuels such as soybean oil, biodiesel (soybean oil methyl ester), rapeseed oil and rapeseed oil methyl ester (RME) can provide both improvement in viscosity at high treat rates and, as shown by Sivebaek et al., at low levels can provide adequate lubricity. What must also be considered in any attempt to formulate a fuel grade DME that possesses diesel-like fluid properties is the practicality and availability of additives and blending agents. Plant oil-derived fuels may need to be blended at rather high levels to provide an adequate boost to the viscosity of DME, but they are commercially available on sufficiently large scale to be practical. Other additives may not be available in quantities that are sufficient to permit production of fuel grade DME. What remains is a need to engineer solutions that provide a large improvement to the viscosity of DME at levels typical of fuel additives, not fuel blending stocks, but that can be produced in sufficiently large volume.

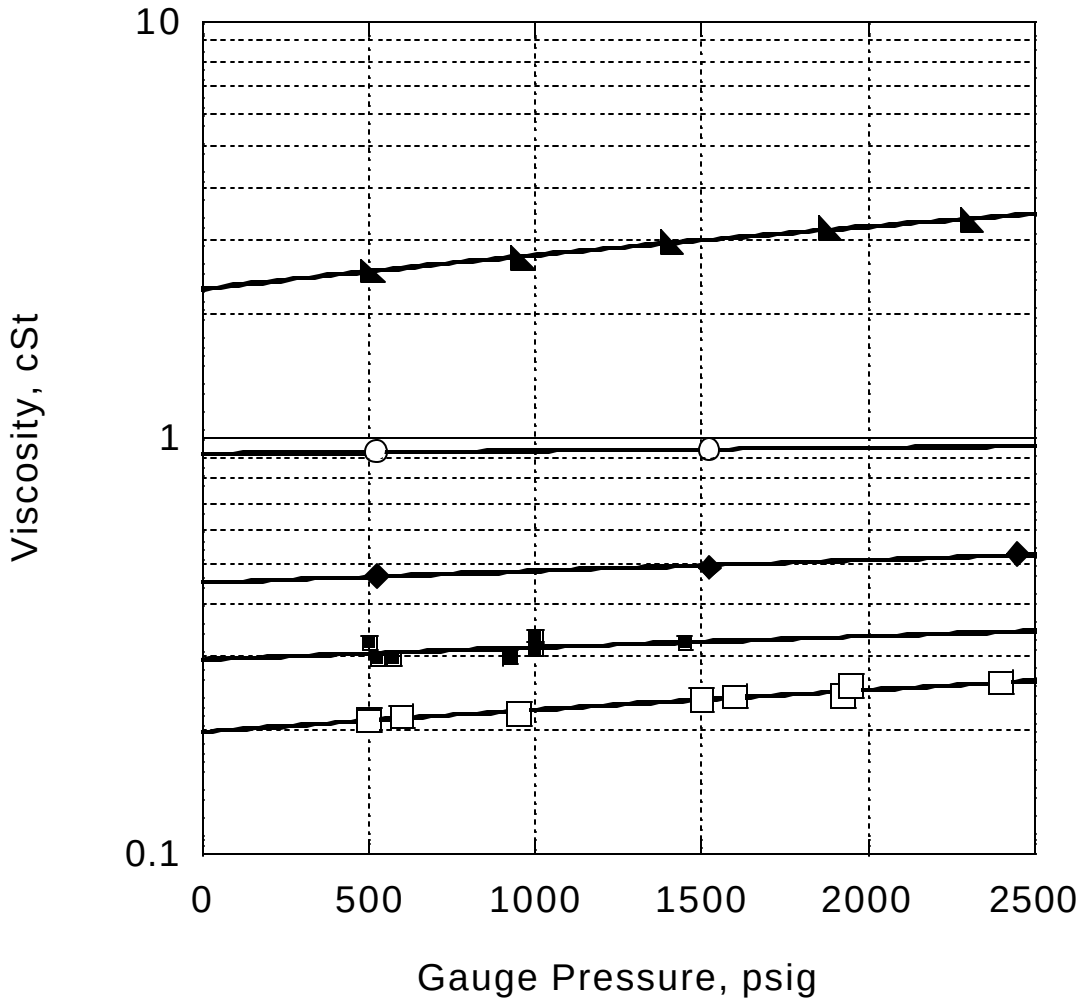

Fig. 7. Viscosity of DME-diesel blends at pressures from 500 to 2500 psi. (◣) diesel fuel, (□) DME, (○) 25 wt.% DME, (◆) 50 wt.% DME, (■) 75 wt.% DME.

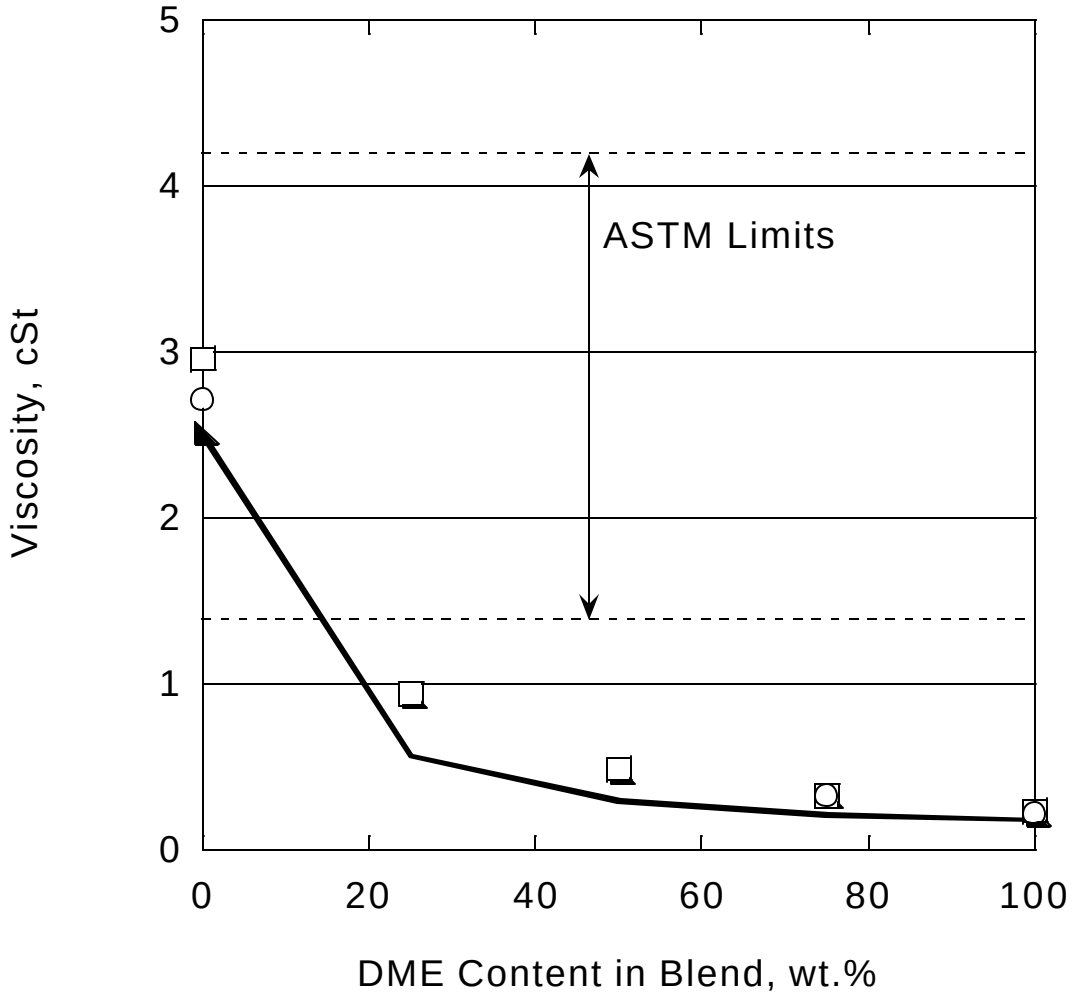

Fig. 8. Blend response of viscosity to DME addition at various pressures. (◣) 500 psi, (□) 1000 psi, (○) 1500 psi, (-) ASTM D 341 blend prediction.

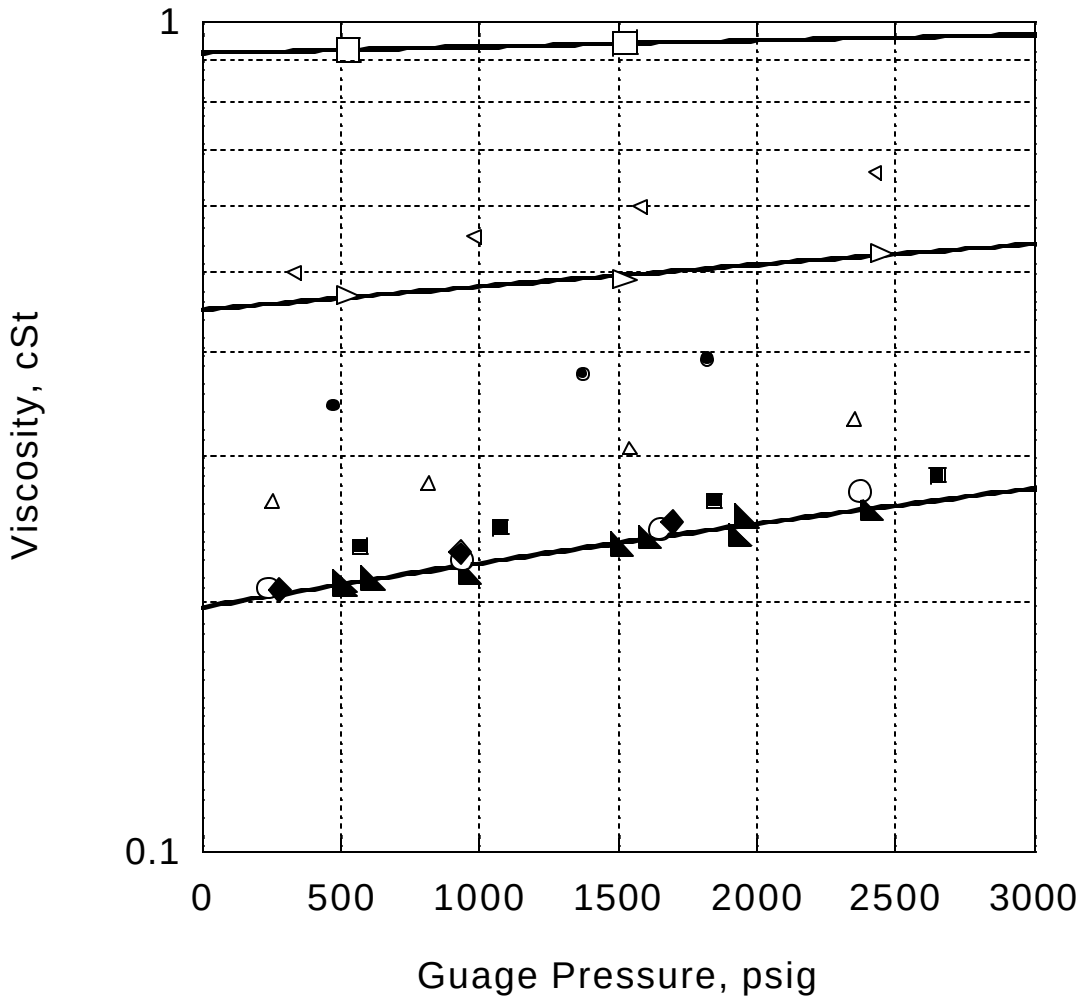

Fig. 9. Viscosity of DME-Biodiesel blends at pressures from 500 to 2500 psi. (◣) DME, (○) 1000 ppm Biodiesel, (◆) 5000 ppm biodiesel, (■) 1 wt.% Biodiesel, (△) 5 wt.% Biodiesel, (●) 20 wt.% Biodiesel, (◁) 50 wt.% Biodiesel, (□) 25 wt.% DME in diesel fuel, (▷) 50 wt.% DME in diesel fuel.

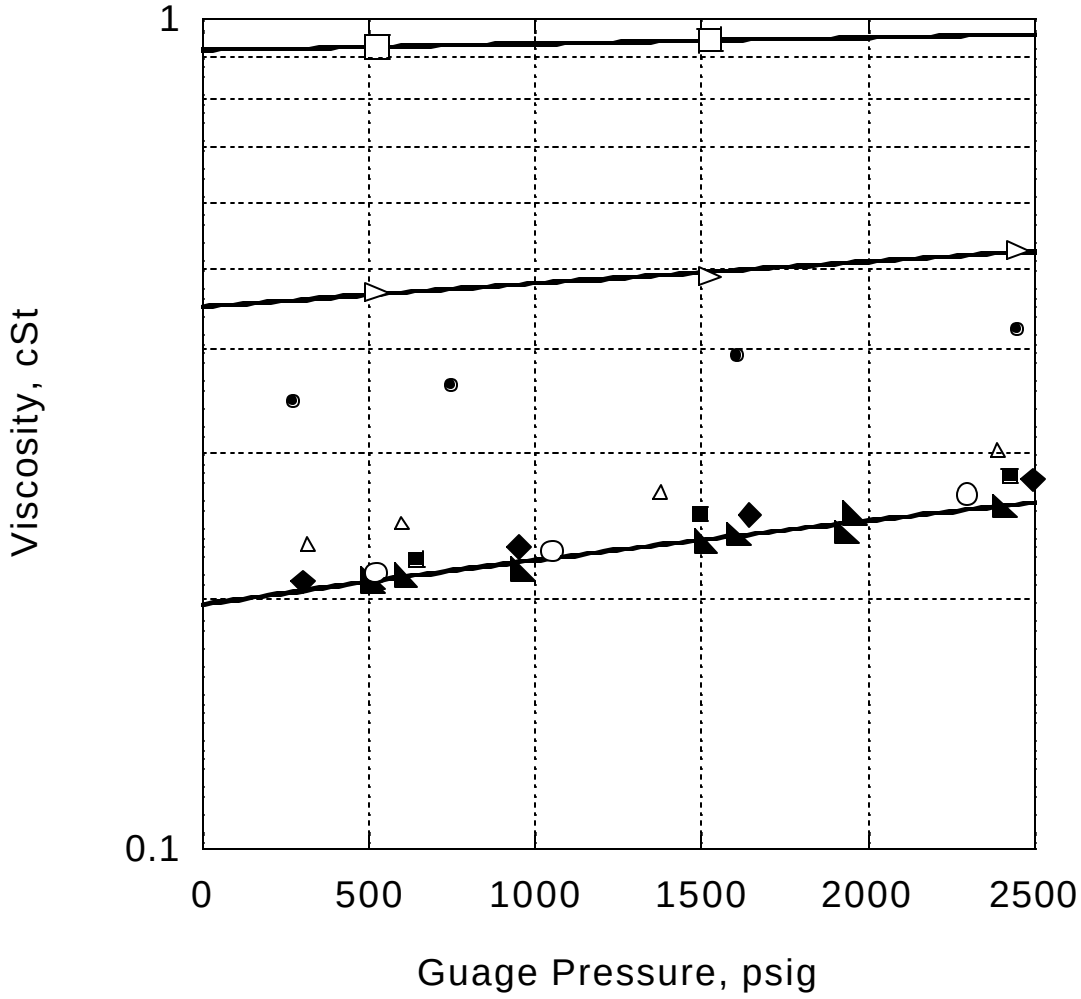

Fig. 10. Viscosity of DME-Soybean Oil blends at pressures from 500 to 2500 psi. (◣) DME, (○) 1000 ppm soybean oil, (◆) 5000 ppm soybean oil, (■) 1 wt.% soybean oil, (△) 5 wt.% soybean oil, (●) 20 wt.% soybean oil, (□) 25 wt.% DME in diesel fuel, (▷) 50 wt.% DME in diesel fuel.

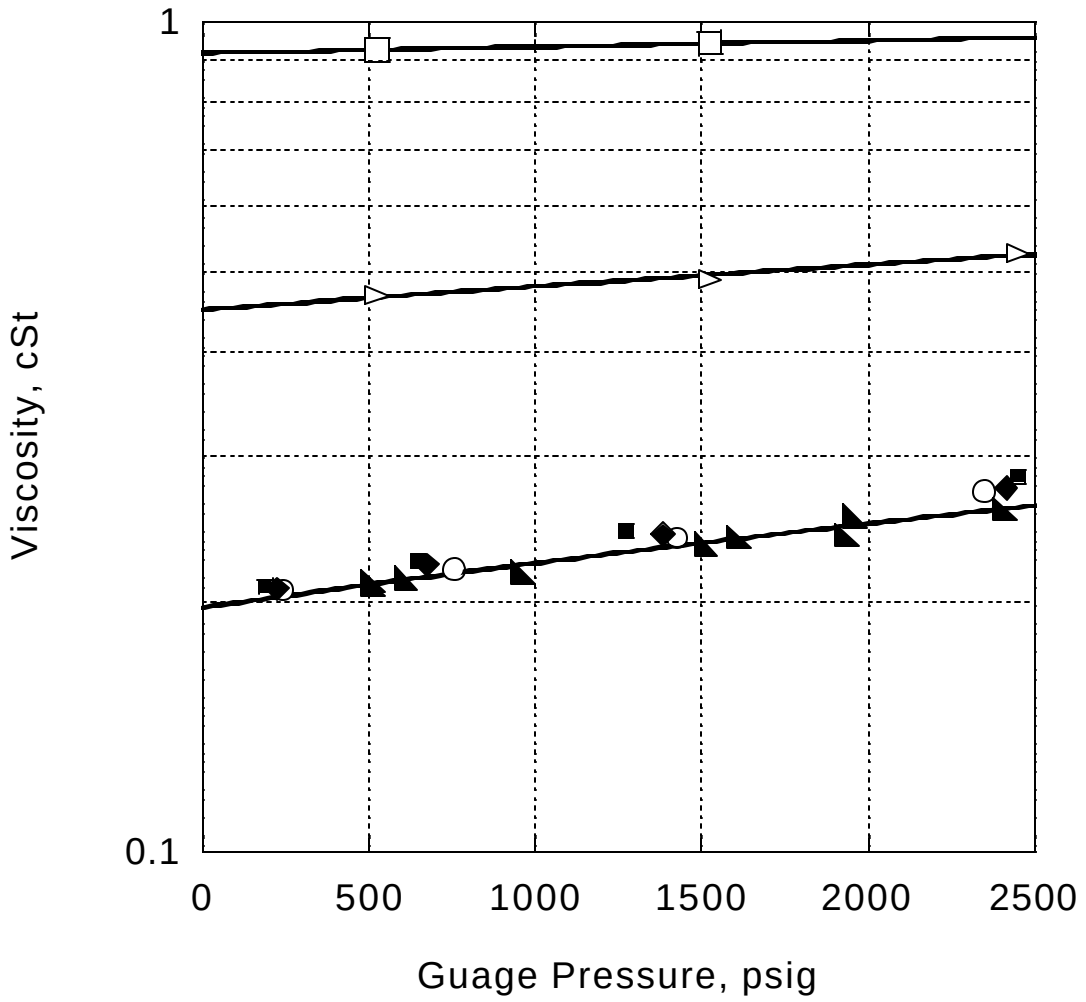

Fig. 11. Viscosity of DME with Ethyl H4140 additive at pressures from 500 to 2500 psi. (◣) DME, (○) 1000 ppm H4140, (◆) 5000 ppm H4140, (■) 1 wt.% H4140, (□) 25 wt.% DME in diesel fuel, (▷) 50 wt.% DME in diesel fuel.

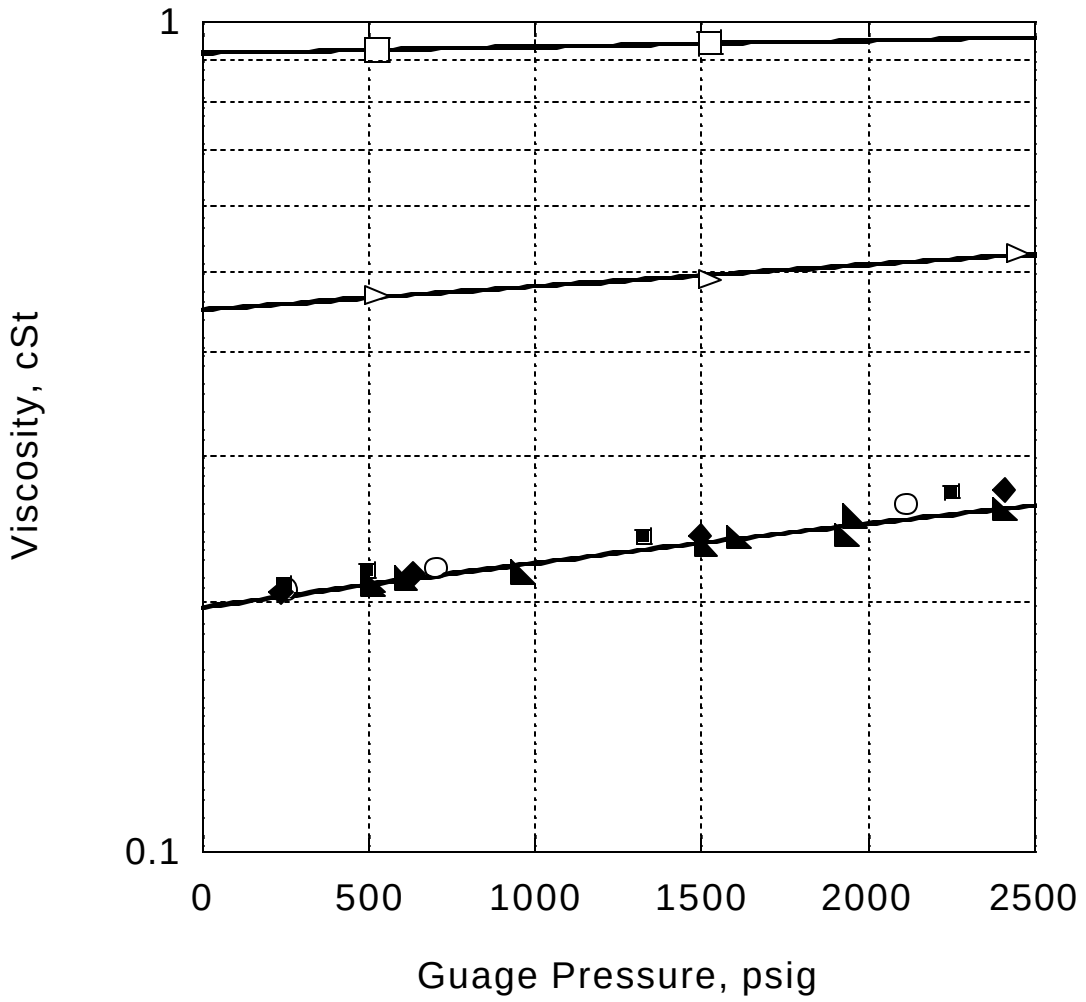

Fig. 12. Viscosity of DME with Ethyl H580 additive at pressures from 500 to 2500 psi. (◣) DME, (○) 1000 ppm H580, (◆) 5000 ppm H580, (■) 1 wt.% H580, (□) 25 wt.% DME in diesel fuel, (▷) 50 wt.% DME in diesel fuel.

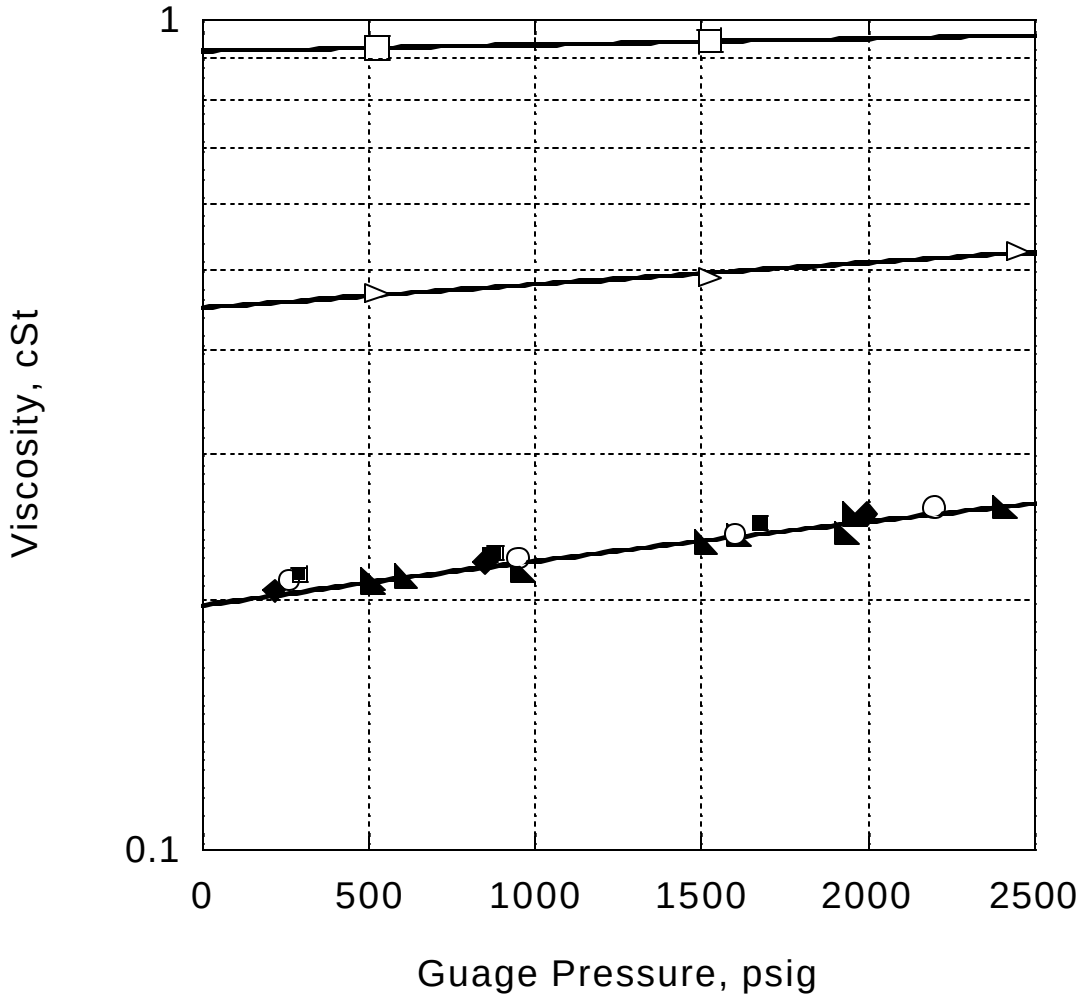

Fig. 13. Viscosity of DME with Lubrizol 539N additive at pressures from 500 to 2500 psi. (◣) DME, (○) 1000 ppm 539N, (◆) 5000 ppm 539N, (■) 1 wt.% 539N, (□) 25 wt.% DME in diesel fuel, (▷) 50 wt.% DME in diesel fuel.

Novel Viscosity Measurements at Moderate Pressure

One of the key properties defining the lubricating ability of a fuel is its viscosity. Several critical engine components, including the fuel pump and injectors, rely exclusively on the fuel to minimize metal contact and subsequent wear. When investigating the benefits of alternative fuels, it is necessary to compare viscosities to a traditional diesel fuel, and to the recommended limits set by ASTM. This chapter details the work preformed with several alternative diesel fuels and a series of additives. The instrument operation is discussed, along with an analysis of the effect of pressure on viscosity.

Introduction. A liquid's ability to properly lubricate a contact in the hydrodynamic and elastohydrodynamic regimes is dependent on fluid viscosity. In the case of diesel fuel, definite limits have been set by the American Society for Testing and Materials (ASTM) test number D 975. When alternative fuels are explored, viscosity is typically compared directly to the same standard.

For this study, three alternative fuels were tested: ultra low sulfur diesel, biodiesel and dimethyl ether (DME). Data exists for all three raw fuels in the literature. In fact, ASTM has created a biodiesel specification, D 6751, designed to qualify biodiesel fuel independently. Dimethyl ether is a far more difficult fuel to work with. It is a gas at standard temperature and pressure, creating a new set of measurement challenges. This high volatility, and extremely low viscosity, are considered detrimental, and thus few published works address DME as a diesel fuel substitute. Two groups have made some progress measuring and understanding DME viscosities. Sorenson, of the Technical University of Denmark, devised a test rig that simulated fuel injection equipment [34]. The test matrix consisted of three lubricity additives in pure DME typically at concentrations of <900 ppm. In all cases, significant wear was observed after 80 hours of operation. A follow-up study in 2001 presented data from a volatile fuel viscometer [25]. Here, a glass capillary viscometer was enclosed in a pressurizable housing and tested with DME and a series of viscosity improving additives. Although improvement was seen, none of the additives brought DME up to the necessary ASTM minimum level.

In a more recent study, Bhide et al. utilized a high-pressure capillary viscometer to study DME-diesel blends at pressures up to 3500 psig [2]. It was found that minimal change in viscosity occurred as pressures were increased from 0-2500 psig. Blends of DME-diesel with greater than 50 wt % DME were not able to meet the ASTM requirement, even at high additive concentrations. This study will expand on this result.

Commercially, several different types of lubricity additives are available. Traditional diesel fuel additives contain a polar group that is attracted to metal surfaces, causing a thin protective film to form. The film acts as a boundary lubricant when metal-metal contact occurs. Two additive chemistries, fatty acids and esters, are commonly used in the range of 10-250 ppm [**Error! Not a valid link.**].

Traditional viscosity-improving additives are classified into several categories including olefin copolymers and polymethacrylates. Olefin copolymers, or OCPs, are comprised of ethylene and propylene, along with a nonconjugated diene in some cases. Polymethacrylates are linear

polymer chains with short, medium or long hydrocarbon side chains that serve to aid solubility. Additives of this type effect the viscosity of a liquid at higher temperatures. In an ambient environment, viscosity additives are generally in a coiled form having little interaction with the bulk fluid. As the temperature is raised, energy is imparted to the coils, allowing them to relax and uncoil. At this point, a noticeable thickening of the test fluid is observed. A challenge with this additive class is shear stability. Long polymer chains are highly subject to shearing in harsh environments. Balancing chain length with the viscosity needs and shear strength is continually a burden.

A second class of additives are organic friction modifiers (OFMs). Friction modified surfaces contain lubricant films built up of closely packed orderly arrays of multimolecular layers, loosely adhering to each other with the polar head anchored to the metal surface. Molecules are generally long and slim with straight hydrocarbon chains of at least 10 carbon atoms and a terminal polar group. The polar group is the governing factor in effectiveness of OFMs. Typical molecules include carboxylic acids, amides, imides, amines, phosphoric acid derivatives and other organic polymers such as methylacrylates.

These two additive types were explored in alternative fuels via capillary viscometry in the following sections. A novel instrument design and more complete test matrix provide valuable insight into the viscosity questions surrounding DME.

Fuels and Additives. As mentioned previously, viscosity testing utilized three primary fuels; ultra low sulfur diesel fuel (ULSDF), biodiesel and dimethyl ether (DME). The fuel properties are presented in Table 2:

Table 2: Alternative Diesel Fuel Properties for Viscometry

	Ultra Low Sulfur	**Biodiesel**	**DME**
Components	Distillate	Soybean Oil	CH_2-O-CH_2
Specific Gravity (15^{o}C)	0.8374	0.930	0.66
Viscosity (cSt)	2.5 @40^{o}C	4.12 @40^{o}C	0.185 @40^{o}C
Flash Point (^{o}C)	63.9	112	-42
Sulfur Total	15 ppm	<31 ppm	0 ppm

The seven additives chosen represent the range of available and applicable blending components. Additives were limited to purely hydrocarbon structures and oxy- compounds. Sulfinated, phosphated and metallo- compounds are inappropriate for combustion systems. The additives and relevant structural and viscosity information are listed in Table 3:

Table 3: Additive Properties for Viscometry

	Structure Type	Viscosity @ 25°C (cSt)	Viscosity @ 40°C (cSt)
Ethyl 5710	Polymethacrylate	22,188	7,585
Ethyl 5751	Olefin co-polymer	34,611	14,093
Ethyl 5777	Ethoxylated long chain alcohols	110,085	33,213
Polycal H-105	High erucic acid rapeseed oil	3,079	1,128
Polycal H-107	Mixed fatty acids	41.9	24.66
Mobil SHF-403	Poly-α olefin	954	398
HT Soybean Oil	Heat modified (polymerized) soybean oil	1,677	708

All of the chosen additives have viscosities well beyond the ASTM required 1.9-4.1 cSt range for diesel fuel. The intent is that such a high individual viscosity will enable a small amount of additive to have a significant impact on the blend. In fact, the viscosity of pure DME is so low, a whole order of magnitude below diesel, that very high additive viscosities are necessary.

Operational Information. The experimental procedure is fully detailed in Chapter 3, however there are several finer points that require a short review to better understand the data set. The instrument is a pressurizable glass capillary viscometer with an adaptable Swagelock® fitting at the fill port. To fill with DME, the entire instrument was cooled in a dry ice-acetone bath and the added volume of DME determined by weight difference. Two variations of the viscometer design were utilized, one with a straight glass channel to the fluid bulb and one with a curved channel. Each instrument was calibrated separately, although there was no difference in tested fluid viscosities between the two. Since the body of the instrument was glass, under an internal pressure of <150 psi due to DME, a safety pressure test was performed. A glass bulb with the same neck structure was tested with nitrogen up to 800 psi without incident.

The chosen test conditions included viscosities are at 25 and 40°C with final viscosities calculated from an average of 10 repeat runs. The test matrix included DME-ultra low sulfur diesel (ULSDF) and DME-biodiesel blends at 25, 50 and 75 wt% DME, pure DME, biodiesel and LSD, and 25 wt % DME blends with either 1 or 5 wt % additive in ULSDF or biodiesel. The 1 wt % additive concentration was chosen to represent the maximum that is economically feasible for a fuel additive. Any further additions would be cost prohibitive. The 5 wt % concentration is a saturation condition, chosen to represent an additive over-loaded environment. These two data points allow for interpolation or extrapolation to other concentrations of interest.

Viscometer constants were determined using Cannon Standard #4 (ν_{40C}=0.409 cSt and ρ_{40C}=0.617 g/ml). Knowing the flow time of the standard through the capillary and the actual viscosity, the viscometer constant is obtained by dividing the two. The viscometer constant is not a function of temperature, only the geometry of the capillary. The viscometer constant for

the straight necked instrument is C_{st}=0.00202 cSt/sec, and the curved neck viscometer constant is C_{cr}=0.00225 cSt/sec.

Also of concern is the solubility of the additives in DME. DME itself is difficult to work with, so the next larger hydrocarbon, diethyl ether (DEE), was used as a screening liquid. Solubility in DEE does not confirm DME solubility, but if an additive is not soluble in DEE, it will certainly not be soluble in DME. The device used was a Babcock bottle; a small glass bulb with a long graduated neck holding about 50 ml of total liquid. Forty-five ml of DEE was added to a bottle, the last 5 ml was the additive in question. The bottle was corked, shaken and allowed to stand for 24 hours. Any separation would be visibly accessible in the graduated portion of the vessel. All additives were found to be soluble up to 5 vol %.

Viscosity Results. The results for the DME-ULSDF and DME-biodiesel blends are shown in Figure 14:

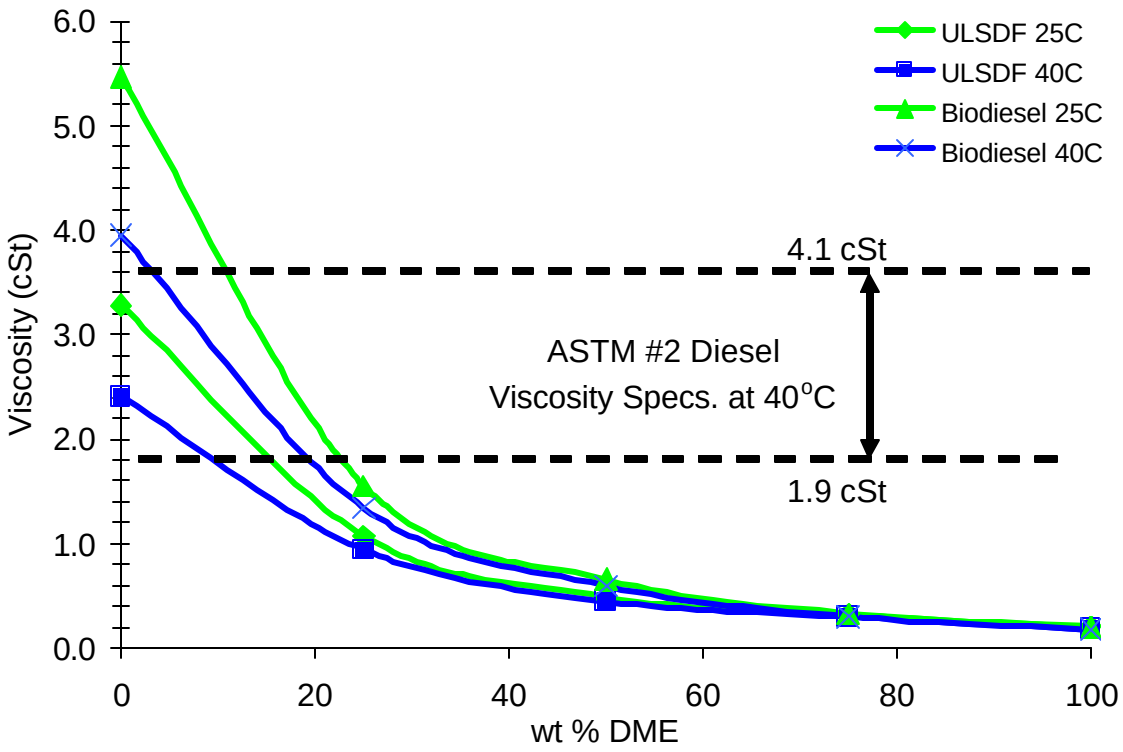

Fig. 14: Viscosities of DME blends in low sulfur diesel and biodiesel fuels

The most striking feature of the graph is the initial drop in viscosity of both ULSDF and biodiesel with very small additions of DME. The 40°C ASTM spec on the chart refers only to the data sets marked with squares or with "x"s. Notice that after about 10-15 wt % DME, the blended fuel viscosity is already below the lower specification limit. Biodiesel has a naturally higher viscosity than ULSDF, but is not capable of offsetting the effect of DME at higher concentrations. This is detrimental to fuel performance and should be enhanced to prevent wear.

Since the 25 wt% DME blends are already below the specification, they were targeted for viscosity enhancement. If a suitable additive was found, it could then be applied to higher DME concentrated blends. Figure 15 summarizes the data from all the additives studied:

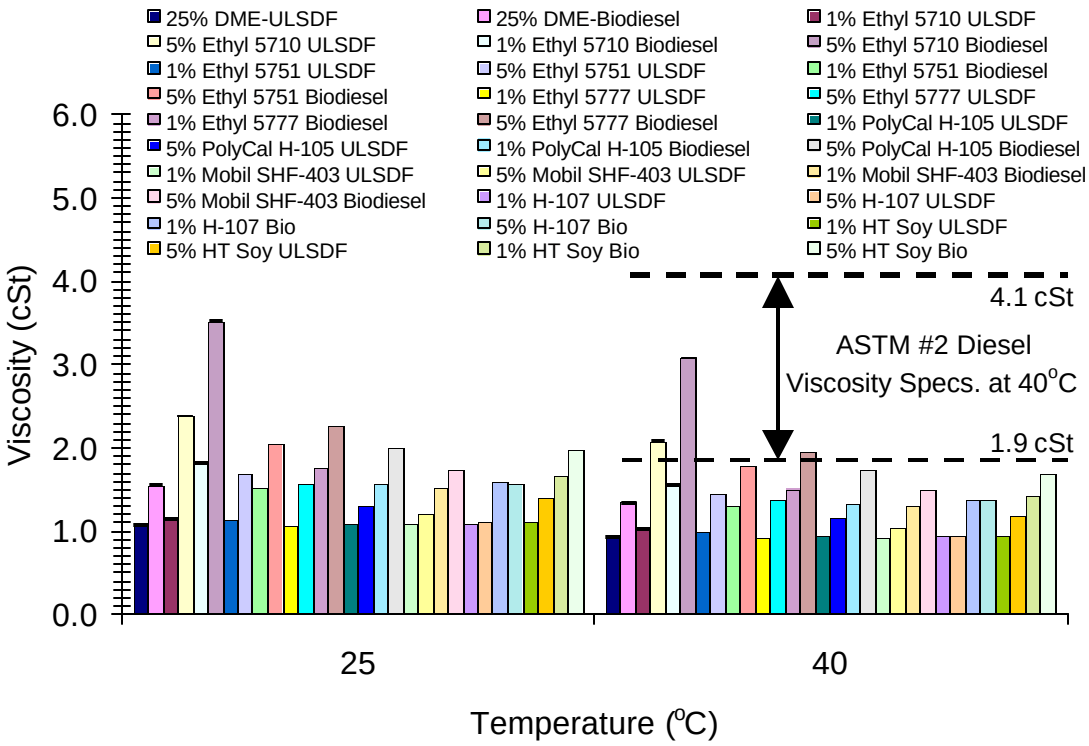

Fig. 15: Viscosities of 25 wt % DME blends with additives

Here the solid bars represent blends of 25 wt % DME in ULSDF, while the hatched bars represent biodiesel blends. For reference, the raw blends of DME, ULSDF and biodiesel as shown as the first two bars in each temperature series. Error bars are shown, however they account for only ± 2% of the final value are undetectable. The ASTM viscosity specification is placed over the 40°C data set for reference. There is no specification at 25°C. Of all the additives tested, only 3 meet the requirement; Ethyl 5710 at a 5 wt % concentration in ULDSF and in biodiesel, and 5 wt % Ethyl 5777 in biodiesel. Ethyl 5710 is a polymethacrylate and 5777 is an ethoxylated long chain alcohol. Both types of additives have very long polymer chains allowing extensive interaction with the bulk fluid. In all cases, viscosity decreased with an increase in temperature, but the rate of change with diesel fuel and DME are not the same. Although there is no viscosity specification at higher temperatures, DME blends may still not offer appropriate protection even if the 40°C specification is met.

The above results assume that kinetic energy, E, is not a factor when measuring flow times. In fact, when a fluid viscosity is extremely low, a correction term must be applied to get correct viscosity values. In general, most viscometers do not require a correction for viscosities above

1.5 cSt, and in some cases, measurements below 0.3 cSt may not need adjustment [98]. In fact, liquids with Reynold's numbers between 80-500 are those that are suspect to a kinetic energy correction. For pure DME, the Reynold's number is 427 in the straight capillary model and 457 in the curved model. This works out to a correction of E=3.57 cSt/sec^2, which adjusts the viscosity of DME from 0.203 cSt to 0.202 cSt, or 0.17%. This is insignificant to the final value as operator repeatability is only ± 2%. All blends and additized fuels will have longer flow times and therefore higher viscosities, driving the kinetic energy correction to zero.

In order to more effectively utilize the viscosity information, a predictive equation would be useful. ASTM has devised such a correlation for petroleum products in Appendix X.2 of ASTM D 341. At 40^{o}C, Eq. 4 is said to apply:

$$\text{Volume of high viscosity component} = \left[\frac{(E-A)(C-D)}{(E-F)(A-C)}+1\right]^{-1} \quad \textbf{(4)}$$

Where:

A = log log $Z_{B(40)}$
B = log log $Z_{B(100)}$
C = log log $Z_{L(40)}$
D = log log $Z_{L(100}$
E = log log $Z_{H(40)}$
F = log log $Z_{H(100)}$
Z = (cSt + 0.70)

Subscripts:
B = Blend
L = Low viscosity component
H = High viscosity component)
(40) = 40^{o}C
(100) = 100^{o}C

The equation can be used if one knows the viscosity of each of the raw components at two temperatures. One can guess the viscosity of the blend, and calculate the volume ratio of each component. This loop can be iterated by adjusting the blend viscosity until the necessary volume ratio is obtained. No specific low viscosity fuel correlations for blending have been developed. This method is compared to the data for DME-ULSDF and DME-biodiesel blends in Figure 16:

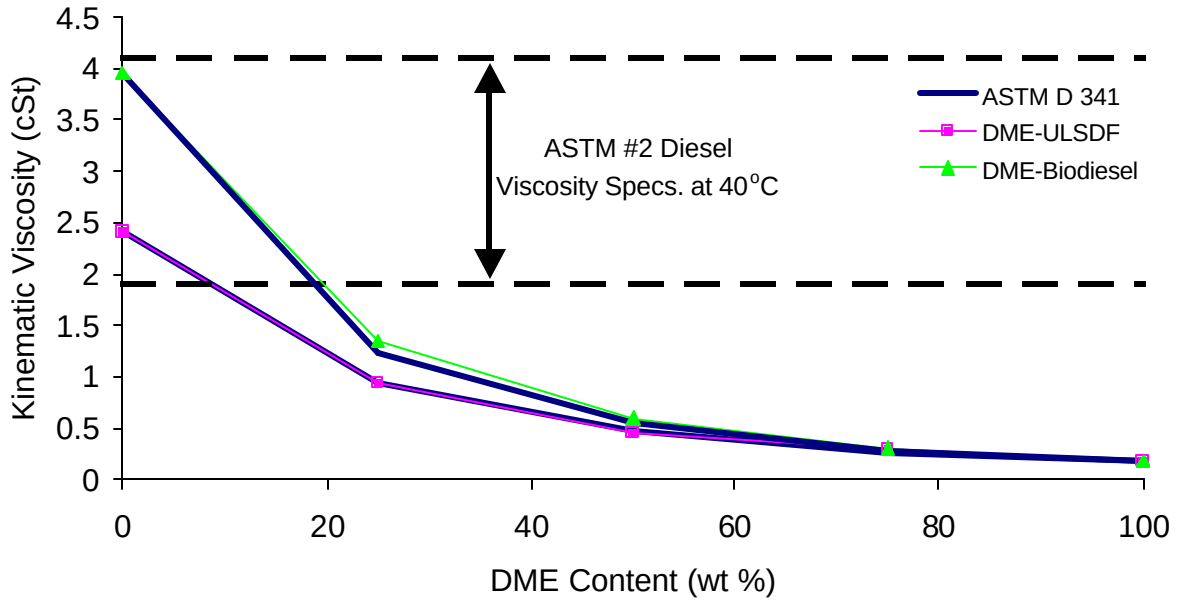

Fig. 16: ASTM blending correlation compared to experimental data for DME mixtures at 40°C

As shown, the ASTM method does a reasonable job predicting blend viscosities. There is no more than a 10% difference between the correlation and the actual measured value. Using this method in the reverse manor, to predict the necessary additive viscosity, a 1 wt % blend ratio in pure DME yields a calculated viscosity of $1 \cdot 10^{45}$ cSt at 40°C to meet the ASTM low viscosity limit. This is an extremely high viscosity; manufacturers do not typically market additives in this range. The shear strength of such an additive would be extremely low due to excessively long polymer chains. Therefore, DME as a pure fuel would be difficult to utilize.

TASK 2. INJECTOR DURABILITY STUDIES

This section provides results from the modified Cameron-Plint wear test apparatus that was adapted for high pressure operation and studies of viscosity and lubricity additives. Also, this section summarizes the efforts, which remain incomplete, to fabricate an injector durability test stand at Penn State.

Application of the Cameron-Plint Wear Test Apparatus to Fuel Injector Wear Studies

The effects of alternative diesel fuels and blends were investigated via a novel wear testing device based on a modification of an existing Cameron-Plint wear tester. The goal of this study is to mimic fuel injector wear as closely as possible, including contact geometry and operational speed. Of the fuels studied, dimethyl ether (DME) resulted in the most significant wear, with decreasing ratios of DME in diesel resulting in less severe wear. The most prominent additive from the lower pressure viscosity experiments was also tested, resulting in increased wear. A profilometer was used to quantify the extent of the wear depth. The following subsections detail the specifics of the testing and discuss the results.

The motivation for this testing stems from a need to better understand the compound effects of system operating conditions, geometry, fuel choice and engine demands on the wear of diesel fuel injectors. In the past, several different types of instruments have been used to attempt to distinguish between alternative fuels and blends. Each system has limitations, which raises questions as to the legitimacy of resultant data.

One of the more popular tools for investigating the lubricity of diesel fuels is the high frequency reciprocating rig (HFRR). The accepted procedure is outlined in ASTM D 6079. Essentially, a vibrator arm holding a non-rotating steel ball and loaded with a 200 g mass is lowered until it contacts a test disk which is submerged in the test fuel at the specified temperature. The ball is the rubbed against the disk with a 1 mm stroke at 50 Hz for 75 min.

A second method relies on different geometry. The scuffing load ball-on-cylinder lubricity evaluator (SLBOCLE) is outlined in ASTM D 6078. In this configuration, a load arm holding a non-rotating steel ball is loaded with a 500 g mass until it contacts a partially fuel immersed, polished steel test ring rotating at 525 rpm. The humidity is controlled at 50 % relative humidity for the duration of the test. The specimens contact for 60 sec before the test is ended.

Of the two methods, only the HFRR is easily adaptable for use with volatile fuels, like dimethyl ether. The pioneer in this field, Lacey from the Southwest Research Institute has published studies investigating this effect. In one such SAE paper [89], Lacey contends that DME has very poor lubricity, and only high concentrations of additives reduced the wear to acceptable levels. In a later paper, Lacey modified the HFRR to also have the capability of elevated temperatures, up to 300^{o}C. He found that water content, with is eliminated at temperatures above 100^{o}C, plays a significant role in the wear rate of volatile fuels. A similar paper by Sivebaek and Sorenson [34], proposes additional adjustments to the system, including frequency reduction and a decoupling of the frictional force and the load magnitude.

Although some discrimination between fuels and additives is available in the traditional techniques, none of these systems realistically provides the appropriate contact geometry for a fuel injection system. This can have a significant impact on the performance of a test fuel. The test proposed in this work eliminates this potential problem. The model system for the modified Cameron-Plint, detailed in the Experimental Section, is a hydraulic electronic fuel injector (HEUI). This state of the art injector takes advantage of electronic control systems for precision injection timing, and a hydraulic pressurization system that multiplies in the inlet pressure by 7 times prior to injection. Figure 17 shows a diagram of the injector [101]:

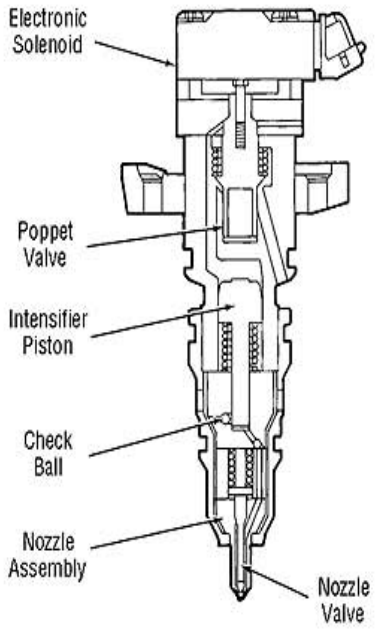

Fig. 17: HEUI diesel fuel injector

The particular area of interest is the nozzle assembly, where a plunger and concentric outer barrel house the fuel prior to injection into the combustion chamber. This novel adaptation of the Cameron-Plint wear tester is a realistic way to account for the geometry and variety of contact conditions during operation.

Fuels and Additives. The bulk of the testing utilized low and ultra low sulfur diesel fuel, biodiesel fuel and dimethyl ether (DME). Blends of these fuels produced a number of different wear conditions. The MSDS sheets for the specific fuels are located in Appendix C. In addition to the fuels, there was also one additive blended into the fuel mixtures. Ethyl 5710 was the best performing additive from the low pressure viscometer tests. For reference, Table 4 lists the most useful properties:

Table 4: Alternative Diesel Fuel and Additive Critical Properties for Wear Test

	Low Sulfur Diesel	**Ultra Low Sulfur**	**Biodiesel**	**DME**	**Ethyl 5710**
Components	Distillate	Distillate	Soybean Oil	CH_2-O-CH_2	Methacrylate Coploymers
Specific Gravity (15°C)	0.8324	0.8374	0.930	0.66	0.893
Viscosity (cSt)	2.482 @40°C	2.5 @40°C	4.12 @40°C	0.185 @40°C	850 @100°C
Flash Point (°C)	63.5	63.9	112	-42	120
Sulfur Total	325 ppm	15 ppm	<31 ppm	0 ppm	n/a
Cetane Number	46.8	49.7	47.6	>55	n/a

Notice the viscosity of biodiesel is much higher than the diesel fuels, as is the flash point. The additive has by far the highest viscosity, as is necessary to impact the very low viscosity of DME.

Operation Information. The experimental procedure for the Cameron-Plint wear tester is detailed in Chapter 3.2. This section will outline the specific performance parameters, justify the operationing conditions, explain the calibration steps taken prior to testing and present a summary of all test specimens.

Test Parameters. Determining the operating and performance parameters required a look at the fuel injector specifications and previous engine test results. The data used for this analysis comes from the MS thesis of E. Chapman [36] and from the HEUI manufacturer. In order to qualify an injector, it must remain stable at heavy loads and high speeds. With this in mind, data from a "Mode 7" test, a high speed and load condition, on a Navistar T444E turbo-diesel engine was used to generate reasonable estimates for injector speeds, volumetric flow rate, timing, etc. Table 5 lists the properties of interest:

Table 5: Fuel injector properties based on Mode 7 engine test

	Value
Engine Speed (/2 to get # of injections/min)	2220 RRM =37 Hz (18.5 Hz)
Volume of Fuel Injected	72.1 mm^3/stroke
Injection Pressure	17.0 MPa
Injection Timing	13.76° before TDC

Using the above parameters, it is possible to calculate the maximum travel distance of the plunger in the barrel. If one rounds up to 80 mm^3/stroke as the maximum volumetric fuel flow rate, and calculates the fuel area using the diameter of the plunger (0.2359", see Experimental section), the maximum travel distance of the plunger is 2.8 mm/stroke. The actual testing condition was set at 4 mm to ensure enough contact between the plunger and barrel. The speed of injection, 18.5 Hz, is easily achievable with the Plint motor. However, in order to accelerate the test, a motor speed of 40 Hz was chosen, more than doubling the number of contacts per second, but not operating at an unsafe speed. The test time was chosen to be 3 hours. This amount of time results in about 500,000 cycles and provides enough of a wear scar to discriminate between samples.

Calibration. In order to determine the correct motor speed, it was necessary to calibrate the digital controller with the actual reciprocating speed of the motor. This was performed with a tool known as a Strobo-tac type 1531-A manufactured by General Radio Co. in Concord, MA. A Strobo-tac utilizes a strobe light with a variable flash frequency. By syncing the rate of the strobe flashing to the camshaft of the motor, one is able to determine the actual speed. This procedure was repeated for several different control settings on the Plint and a calibration curve defined as shown in Figure 18:

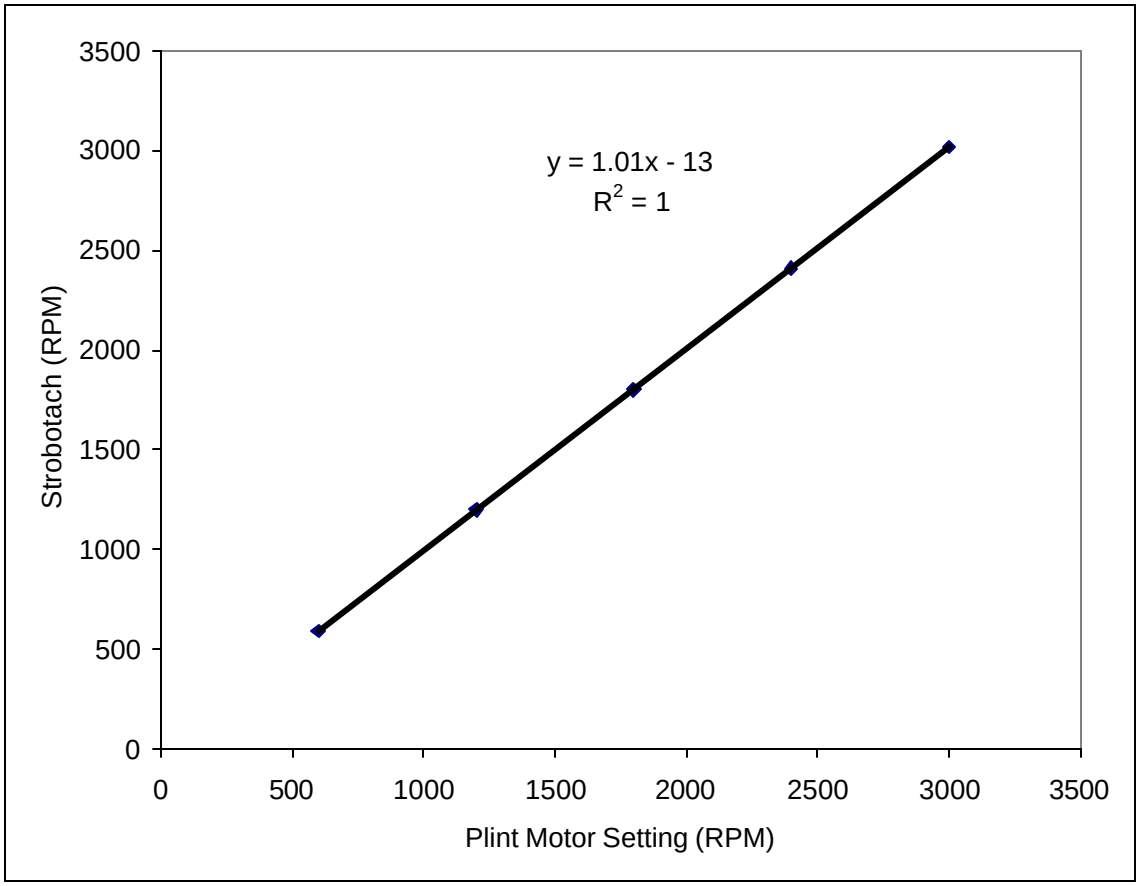

Fig. 18: Plint motor calibration curve

From the graph it is evident that the motor setting is calibrated to a reasonable level. There is a ± 5 RPM error bar on the Strobo-tac measurements, meaning little or no error in the setting of the Plint exists.

Another important piece of information is the upward force on the plunger due to the movement of the motor shaft. This can be calculated with a few additional pieces of information. Figure 19 shows a schematic of the motor configuration for reference:

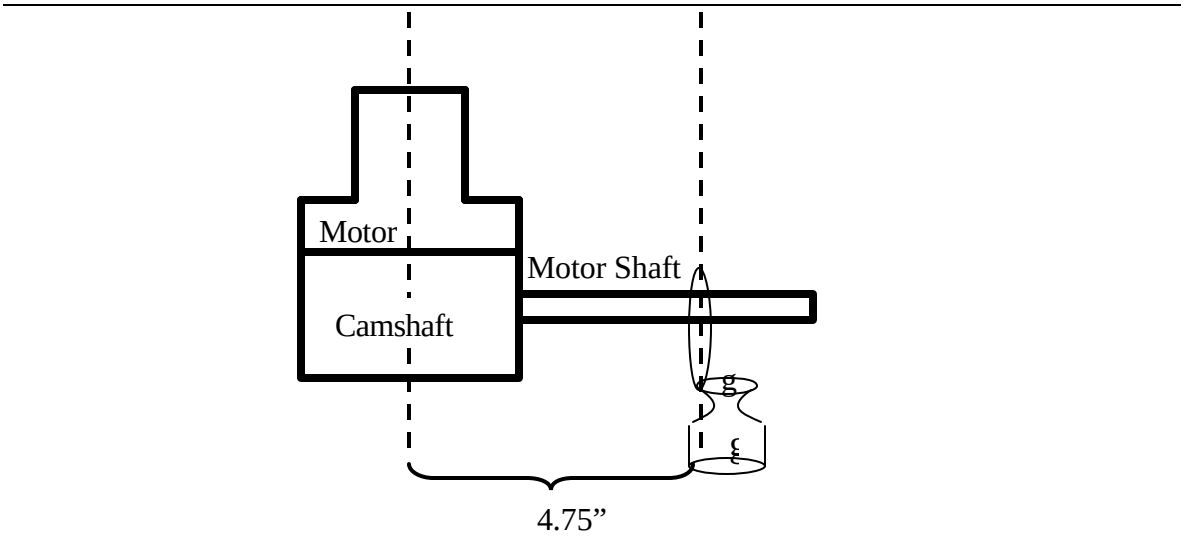

Fig. 19: Diagram of motor configuration for Plint

By setting the motor to the operational speed of interest, 40 Hz, one generates a certain amount of torque. This force can be offset by attaching weights to the end of the shaft, opposing the force pulling the shaft upwards. With the precise amount of weight, it is possible to balance the shaft in a horizontal position. With this weight, and the distance from the center of the camshaft to the measurement point, all the variables in Eq. 5 are known;

$$(T=Fl) \qquad \textbf{(5)}$$

Where ? is torque, F is the opposing force and l is the length. Knowing F and l, the calculated torque is 591.8 Nm. The position of interest is the plunger-barrel contact point located 26 cm from the centerline. At this point the force is 2276 N or 232 Kg. This value represents the maximum possible force applied to the pin in the positive z direction. In reality, the o-rings responsible for the dynamic seal also take up some of the load, resulting in a 3-point contact geometry, but this value does represent the upper bound. Since there is no known relationship for the force distribution across the o-rings, this value is all that is obtainable.

Test Matrix. Only 10 cylinders and 20 pins were machined for the Plint wear tester. The fuels tested included low sulfur diesel (LSDF), ultra low sulfur diesel (ULSDF), dimethyl ether (DME), and biodiesel (Bio). The most successful additive from the viscosity testing in the low pressure viscometer, Ethyl 5710, was also tested. The first several specimens were used to determine the appropriate running time for the test, and are therefore not included in the final result. Table 6 provided details on the test matrix:

Table 6: Plint wear test specimen list

Pin #	Cylinder #	Test Fuel (wt %)
4	4	DME
7	1	LSDF
8	3	LSDF
9	9	LSDF
10	10	ULSDF
11	11	ULSDF
12	12	ULSDF
13	13	75 wt% DME/ULSDF
14	14	30 wt% DME/ULSDF
15	9	50 wt% DME/ULSDF
16	10	75 wt% DME/Bio
17	11	50 wt% DME/Bio
18	12	25 wt% DME/Bio
19	13	25% DME; 70% Bio; 5% 5710
20	14	25% DME; 70% ULSDF; 5% 5710

Test references will henceforth be referred to by pin number. Notice that tests 7-9 and 10-12 were repeats of the same fuel. This is done in order to establish error bars, or statistical significance of each test. Blends with DME were designed to explore the range of fuel blend options and determine if a trend between DME content and wear volume existed. Finally, Ethyl 5710 was blended into 25 wt % DME to determine if the viscosity increase resulted in acceptable wear.

Wear Test Results. There were two primary methods explored for wear characterization. The first was weight loss of the pin-cylinder system during operation. The second method was wear scar depth profiling, obtained using a profilometer. Each of these methods, along with analysis and implications will be explored in this section.

Mass Loss. Prior to each test, the pin and cylinder mass was recorded using a 5 place Sartorius balance. Each specimen was throughly cleaned to remove residue before a weight was taken. After the completion of the test, the specimens were again cleaned and weighed on the same balance. The change in mass was caluclated at plotted in Figure 20:

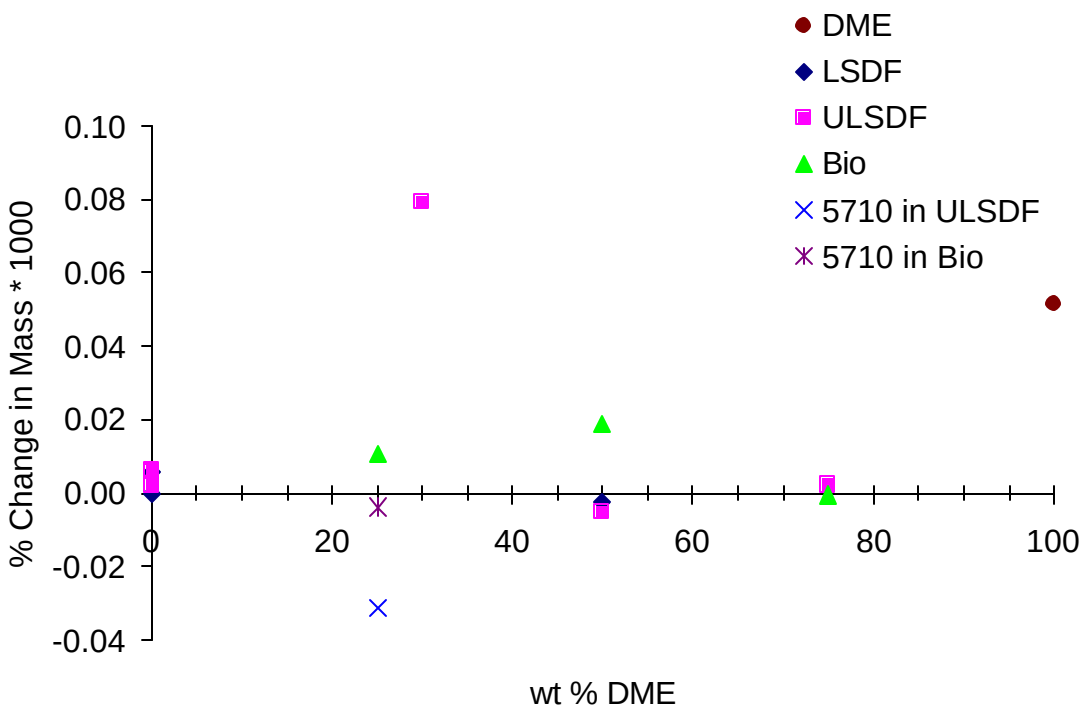

Fig. 19: Total system mass loss during Plint wear tests

From the graph, there are no discernable trends between change in mass and fuel type. In fact, it appears that certain specimens actually gained mass during testing. The most likely reason for this apparent scatter is that a transfer of worn material occurred. Optical examination of the pin specimens reveals a definite worn area on the upper surface (detailed in the next section), therefore a discernable change in mass should be present. The cylinders were not optically accessible, but profilometry later revealed material buildup on several of the pin specimens as shown in Figure 21:

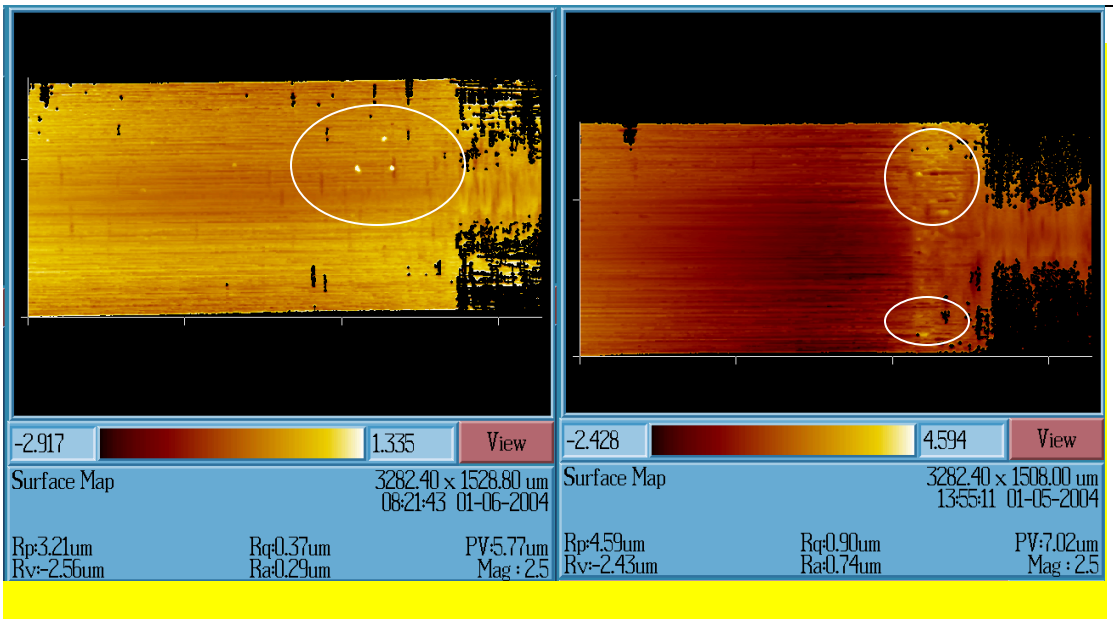

Fig. 21: Pin # 15 and #17 showing material buildup

In the ideal case, if all worn particles were transferred from the pin to the cylinder, the change in system mass should remain zero. In practice, additional foreign particles, e.g. dust, water film, residue, would result in a slightly higher final mass. In certain cases, worn particles may have been freed during the test, resulting in a reduced system mass. This inconsistent property is therefore not the most reliable method of determining wear.

Another possibility for wear measurement is to only look at the pin mass loss. This is not as technically sound as using the entire system mass since both surfaces are most likely being worn simultaneously. The results are presented in Figure 22:

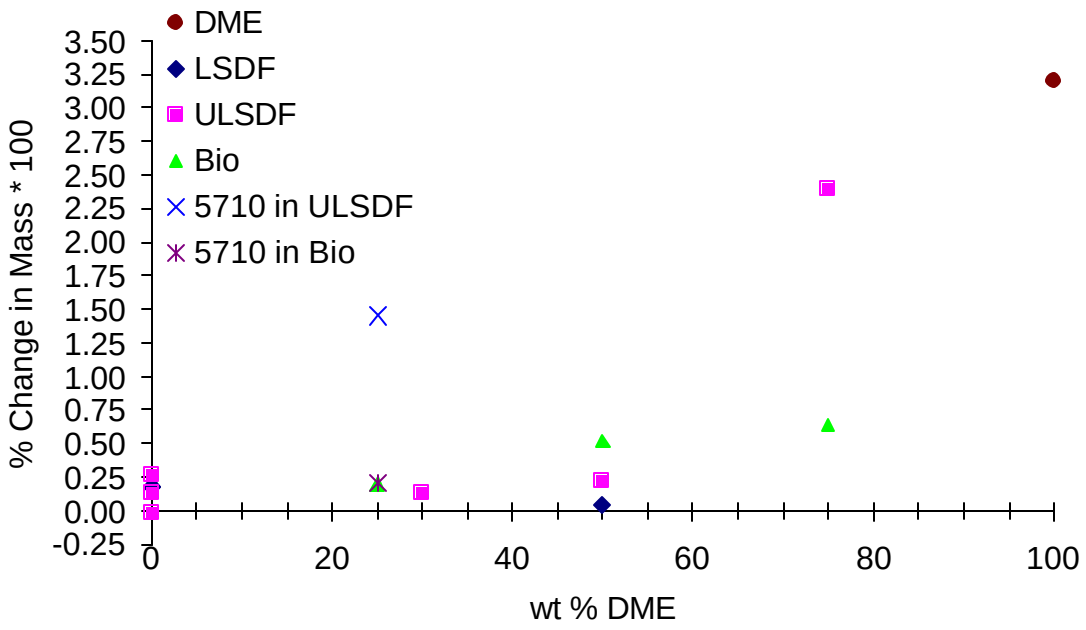

Fig. 22: Pin mass loss during Plint wear tests

The trends in this graph are far more significant that in the previous case. The pure DME case resulted in the highest mass loss, while LSDF and ULSDF blends trended upwards with increasing DME content, as expected. From the graph, it appears that for the ULSDF case, up to 50 wt % DME does not result in dramatic wear over the 500,000 stroke testing cycle. Biodiesel use appeared to significantly reduce the wear at higher DME quantities. The addition of Ethyl 5710 to a 25 wt % DME blend of biodiesel resulted in no significant wear reduction. The same additive in ULSDF actually resulted in a significant wear *increase*, a counterintuitive response. This effect is negated if one looks are the matching outer cylinder, in which significant material loss occurred. As a general rule, using just the pin as a measure of mass loss is an ineffective method of analysis. A more appropriate method, wear scar mapping, is outlined in the next section.

Wear Scar Depth Profiling. In order to provide a concrete method of comparison between specimens, all pins and cylinders were mapped using profilometry. Prior to this imaging technique, optical micrographs and visual inspection revealed the locations of worn areas on the pin surface. The diagram in Figure 23 details the wear regions on the pin specimens.

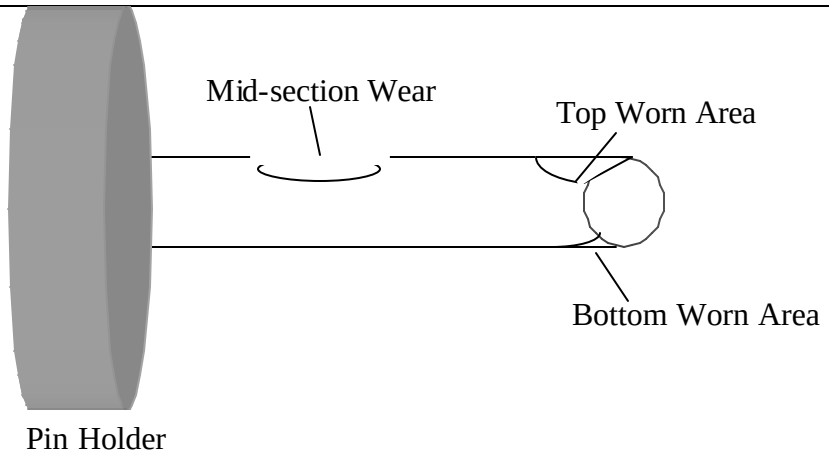

Fig. 23: Diagram of potentially worn area on Plint pin specimen

In all cases, material from the top of the pin was worn away. This is not surprising considering the torque from the motor is imposing a force in the positive z direction. Mid-section wear occurred in most cases as well. The position of the wear scar corresponded with the maximum "in" stroke, the point where the pin is furthest into the cylinder. The lower worn away area was only apparent in a few cases. This is most likely due to collapse of the lubrication layer and direct metal-to-metal contact during the onset of the test.

Optical microscopy yields a visual method of pin inspection. An example of a DME worn pin is shown in Figure 24:

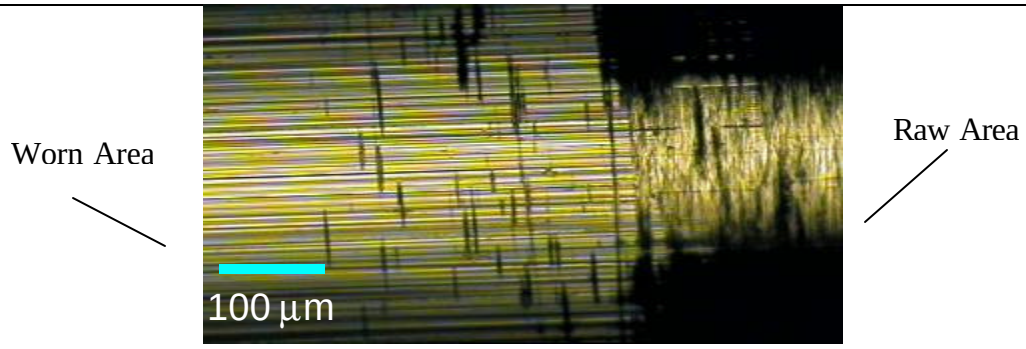

Fig. 24: DME worn pin from Plint wear tester

In the raw, or unworn pin area, only a small portion of the pin surface is visible. This is due to the focal depth of the microscope. On a curved surface, the height is variable and only a certain z range is in focus at any particular time. On the left side however, the surface has been worn away to expose a much flatter area. Notice the polishing marks from the machine shop are vertical, while the wear marks are aligned in the direction of motion horizontally. This is one method of proving that a certain area has been worn away during testing.

The outer cylinders had to be cut in half lengthwise prior to imaging. It was found upon inspection that in all cases, no significant wear marks were present. The majority of the wear occurred on the pins, with only slight material transfer causing a change in the final mass of the cylinders. One possible explanation for this occurrence relates to the actual machining process. The pin surfaces were simply ground to the correct size and roughness, a fairly low energy-intensive process. The cylinders however were wire burned to create the proper inner diameter. This process atomizes material at high temperature, and possibly hardens the metal surface simultaneously. Therefore, the inner cylinder walls may be harder than the pins and less likely to wear.

Profilometry allowed quantification the wear scar characteristics. An example image is shown in Figure 25:

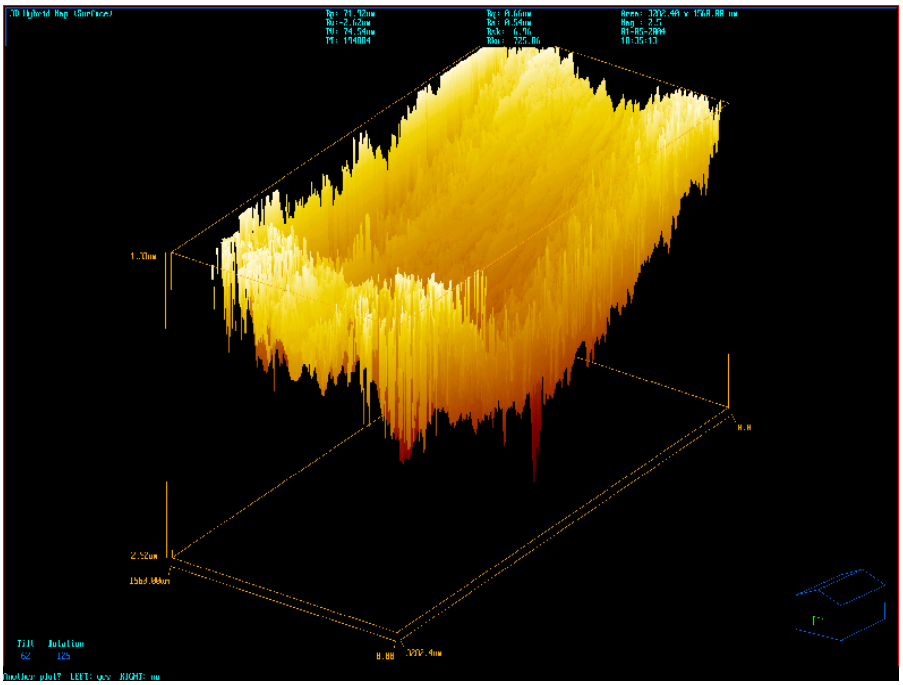

Fig. 25: Profilometric image of wear scar on pin #13 top wear scar

The scooped out portion is missing pin material. The shape has been flattened, to remove curvature, and normalized. The lightest areas represent the tallest features, which are the raw or neat pin heights. Unfortunately, the profilometer is not capable of capturing the entire wear scar in one map. The wear area, even at 5x magnification, is too large for a single image. This inhibits the calculation of wear volume and wear area. The parameter chosen to describe the wear scars is therefore wear depth. In the ideal case, wear depth is directly proportional to wear area and volume.

The data from the profilometer is displayed in Figure 26:

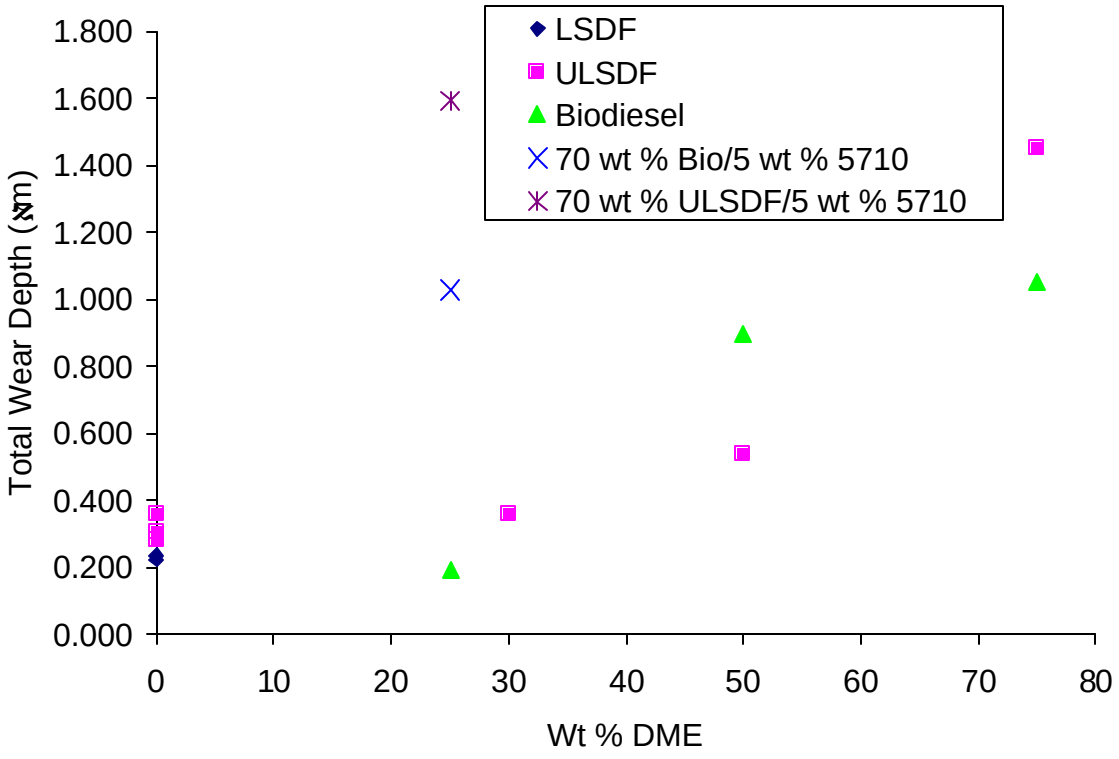

Fig. 26: Total wear scar depth on pin from Plint wear test as a function of wt % DME

Each data point in this graph represents three different line scan measurements at the deepest points in the scar. The average of these points is then compared to the raw unworn height and a total wear depth is obtained. The raw data and the standard deviations of the three measurements take can be found in Appendix E. One set of data was repeated 3 times in order to gauge the repeatability of the test. For the three ULSDF points the average was 0.317 µm deep with a standard deviation of 0.04 µm (13% of the recorded value). For ease of readability, the pure DME data point has been omitted. The wear depth of a pure DME sample was recorded as 6.371 µm.

This method of analysis yields fairly predictable trends. The least amount of wear is observed in LSDF and ULSDF, as expected (raw biodiesel was not tested). As the amount of DME in the blends increases, more wear is observed. At even 25 wt % DME, more wear is seen that with pure ULSDF, unlike the mass loss case. It is interesting to note that the 25 wt % DME/biodiesel blend exhibits extremely good wear resistance. This is likely due to the enhanced lubricity of biodiesel, long known to be superior to diesel fuel. This hypothesis is strengthened by the data at 75 wt % DME. At 50 wt % however, ULSDF actually out-performs biodiesel. If one looks to the shape of the curves made by the ULSDF and biodiesel data points, it becomes apparent that two different mechanisms are at work. For the ULSDF case, the slope is gradual until about 60 wt % DME when it takes on an exponential shape. Biodiesel on the other hand exhibits a steep initial slope and appears to level off around 60 wt % DME. The two functions cross around the 50 wt % DME data point, the reason for the inverted relationship.

The most dramatic features on the graph are the additive data points. In both biodiesel and ULSDF, significantly higher wear occurred than without the presence of the additive. There are several possible reasons for this occurrence. One explanation is that since the same fuel is cycled in the wear tester, and not injected into a combustion cylinder after each compression stroke, the long polymer chain additive may shear apart and become ineffective. The highly polar head group would still preferentially bond to the metal surface, but there would be little or no load support. In fact, a corrosive or oxidative mechanism may work in tandem to further wear the components. The severity of the wear suggests that little or none of the diesel fuel's natural lubricity molecules are able to effectively reach the surface. Notice that again however, biodiesel was the more effective blending agent in the testing.

Unfortunately, there is no established maximum standard for this particular test geometry. If one sets the max just above the wear depth observed for LSDF and ULSDF, then only the 25 wt % DME/biodiesel and potentially the 25 wt % DME/ULSDF blends are effective lubricants for the injection system. Further exploration with additives and other fuel blends may provide a formulation that is effective and environmentally friendly at higher DME concentrations.

Development of an Injector Durability Stand

The Cameron-Plint wear test apparatus described under Task 1 achieves a partial simulation of the wear that can occur within a HEUI fuel injector. The wear component that experiences the reciprocating motion and wears within the high pressure cell is the pin that serves as the Nozzle Valve seen in Figure 27. The pin slides within a cylinder (or barrel) with a very tight tolerance. The wear mechanisms is likely a direct sliding wear between the pin and the cylinder (i.e., a scuffing wear) that is affected by the lubricating quality of the surrounding fluid (hydrodynamic lubrication) and the viscosity of the surrounding fluid (boundary layer lubrication).

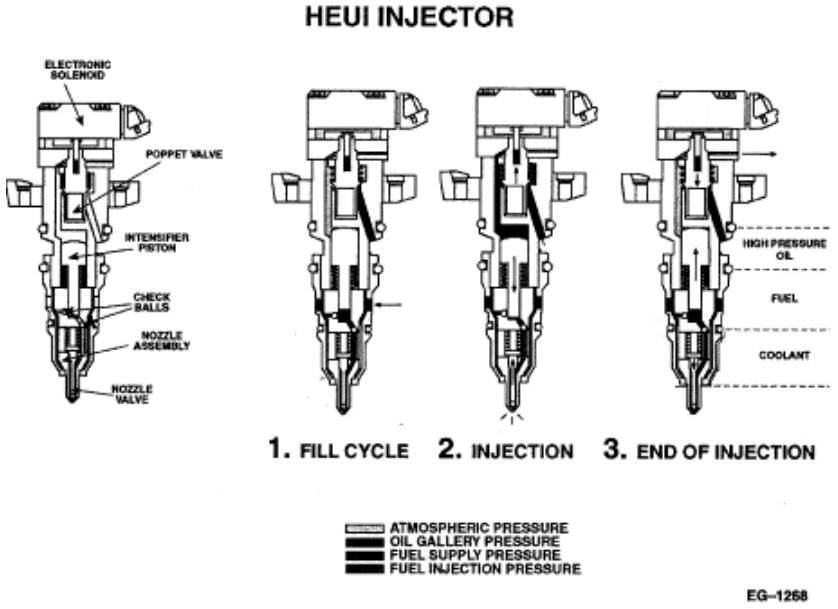

Fig. 27. Schematic Diagram of the HEUI^{TM} Injector

Once lubricity and viscosity improvers have been selected or developed, they need to be tested in actual injectors to assess their ability to delay failure of the injectors through wear. To accomplish the operation of HEUI fuel injectors on test fuel blends and additives, a system is needed to support, operate and deliver fuel mixtures to the injector. At Caterpillar such systems are referred to as Endurance Stands. This injector durability stand was originally going to be fabricated at Penn State with input from Navistar and Caterpillar, both of which have provided support for the DME research at Penn State. However, the cost and complexity of building such a system led to a change in this part of the project plan. Instead of developing an in-house system at Penn State, we began discussions with Michigan Custom Machines (MCM) Inc. who previously built HEUI injector stands for Caterpillar. MCM estimated that a complete stand would cost a minimum of $125,000, but that a simpler stand that had been built for a customer and not delivered could be provided for $30,000. Neither of these prices was compatible with the budget for this project, so a third option was investigated, that of obtaining a donation of a system for use at Penn State.

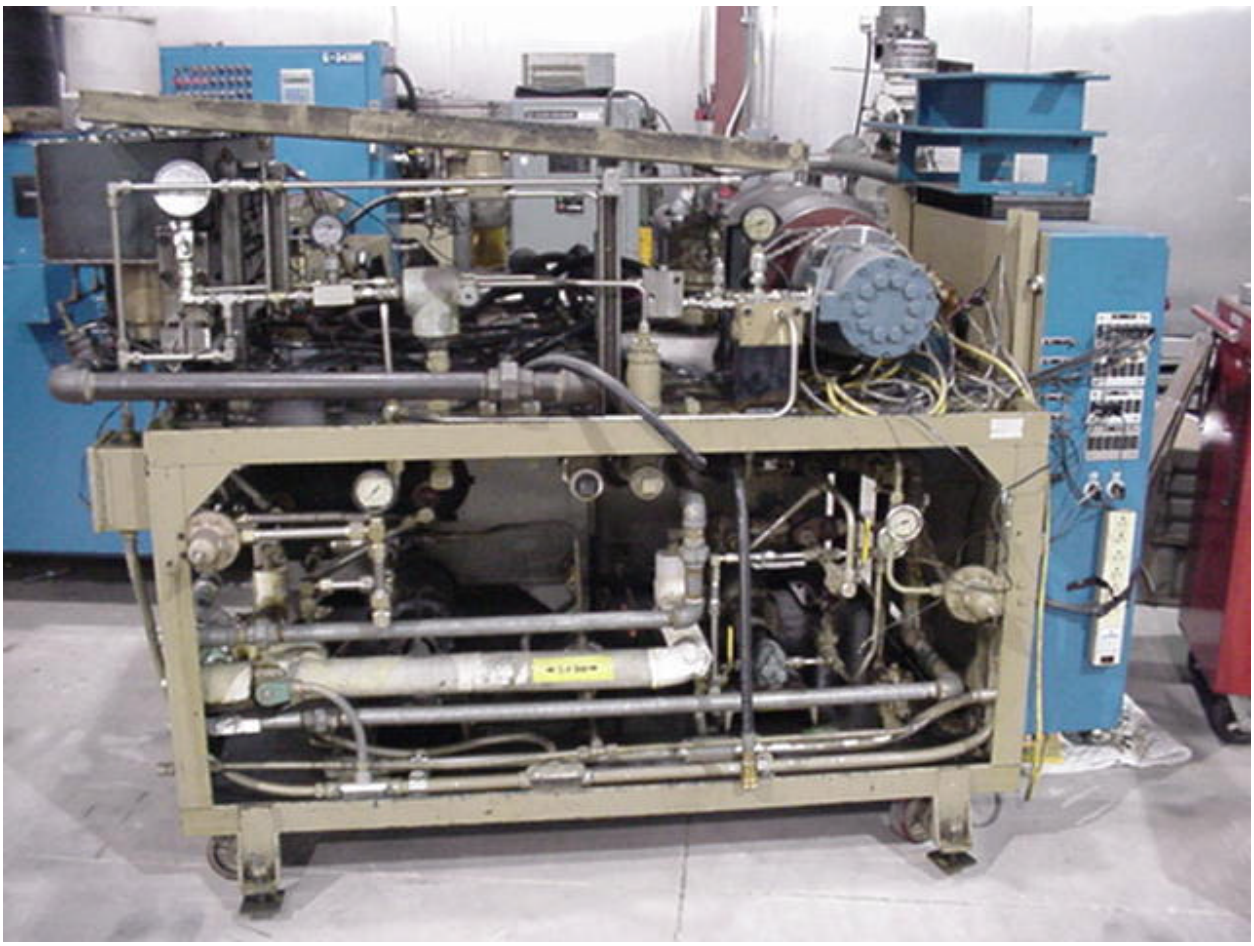

Fig. 28. HEUI Endurance Stand for injector durability studies

So, we approached Caterpillar with a request for a donation of additional equipment, specifically a HEUI Endurance Stand which is shown in Figure 28 (this would have been in addition to their existing commitment to supply fuel injectors and technical services to this project). In response,

Caterpillar informed us early in 2002 that a HEUI Endurance Stand could be donated to Penn State, pending approval by upper management. However, by June 2002 Caterpillar informed us that their management had turned down the request for donation due to changes in the financial picture for their fuel systems unit.

Therefore, we embarked on a process of constructing our own durability stand using student labor and equipment from the DME Shuttle Bus project. Through the Penn State Learning Factory, which brokers senior design projects from Industry and the University for student teams to pursue, we enlisted two senior design teams to develop an injector durability stand. In Fall 2002 semester, a group associated with Mechanical Engineering 414 developed the fluid handling and mechanical design. In Spring 2003, a group associated with Electrical Engineering 403 developed the power and control system design. The final reports submitted by the student teams are inserted below.

ME 414 Summary of Student Design Project Final Report

Through limited research, the Energy Institute believes the engine can operate on DME-diesel fuel blend with up to 28% volume DME. Unfortunately, at this level of mixture, the engine is derated above certain loads as it reached the upper limit of the injector pressure capability. Due to the limited amount of data, it has not been determined if the fuel injectors will allow for higher percentages of DME fuel.

The best way to acquire accurate data regarding the effects of DME on the fuel injector is to simulate the actual fuel injection process. This can be accomplished by creating an apparatus for the fuel injector that can run continuously while simulating actual engine conditions. The goal is to determine the wear characteristics of the fuel injector with low viscosity and low lubricity fuel blends. The Energy Institute has requested three deliverables from Diezel Corp. These include a fuel injector test stand, computer interface to the injector, and documentation.

The design specifications are broken up into the following three categories:

- Fuel Injector Test Stand:
    - Must be able to run continuously to simulate long-term durability effects.
    - Support the fuel injector and the cylinder head.
    - Include fuel and oil systems with specific pressure and temperature regulations.
- Computer Interface:
    - Use LabView to monitor the entire system.
    - Be able to acquire simulation data and store for later analysis.
- Documentation:
    - Create a manual for use of test stand and computer monitoring system.

There were a number of limitations involved with building the fuel injector test stand. The first was the space provided to build that actual stand. The Diesels were given a space about three feet by five feet to build the entire stand. This meant that all components of the stand had to be small and compact, as shown below.

Fig. 29. Fuel Injector Test Stand During Fabrication Process

The Fuel Injector Test Stand was built in the Energy Institute lab at the Academic Activities building. At the present time the stand is not fully capable of running because of a lack of controller modules for the fuel injectors. Once the controller modules are in place the stand should be able to run non-stop for long periods of time. There will be several monitors throughout the system that will shut off the fuel line as well as the injectors if a problem were encountered. Also, all data will be automatically collected through the LabView program. This means little, if any, supervision is required to run the fuel injector test stand.

After sorting the mechanical nature of the test stand, we needed to focus on the data acquisition system. Our team selected a board from national instruments that would suit our needs. Afterwards, we learned that the board was not necessary and that we could actually use existing systems provided by the energy institute. We then needed to create a program in lab-view to collect the data from the stand. A screen shot of our program can be seen below.

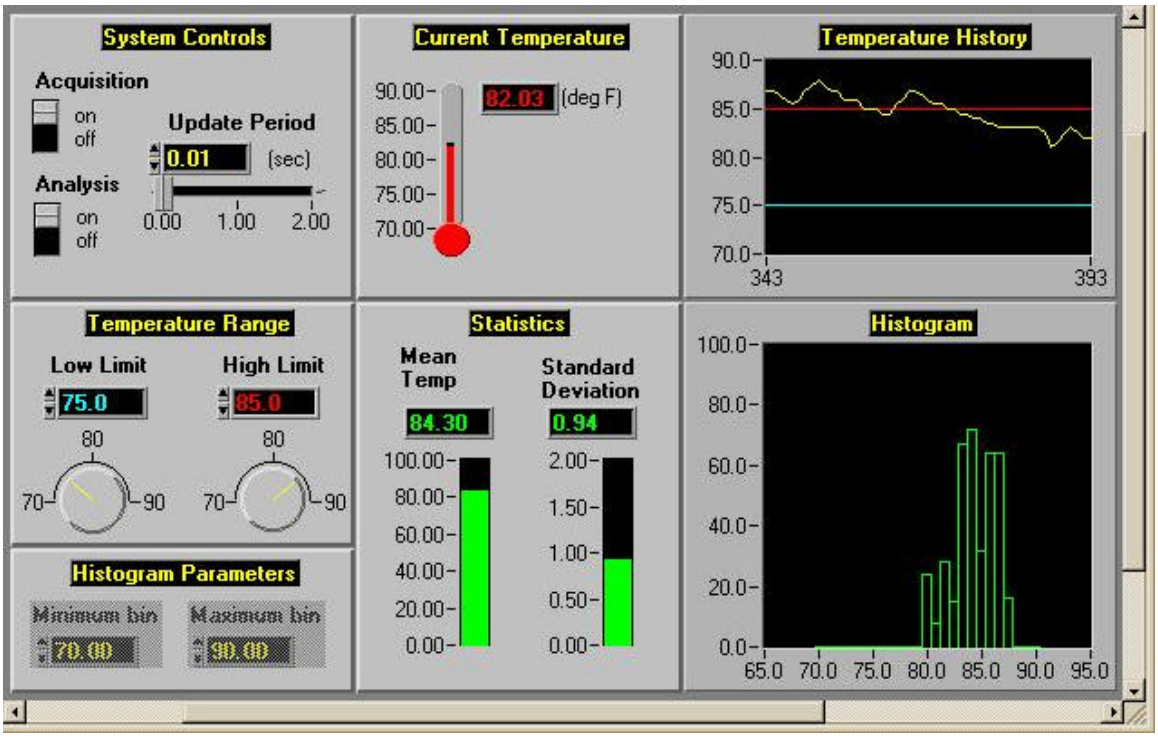

Figure 30. Labview Process Screen for Injector Test Stand.

Summary

Due to the fact that the system is currently incomplete and therefore inoperable, no data has been collected. All of the data acquisition components are in place and ready to run. Once the fuel injector firing control module arrives and the exhaust is assembled properly, testing can be conducted.

EE 403 Summary of Student Design Project Final Report

This project stems from a need to test diesel engine fuel injector durability in a laboratory setting. The design team's task was to create a control system for the fuel injector test stand and to distribute power to the mechanical components.

We used a software program called Lab View to control the operation of the fuel injector test stand and collect the desired data. Power distribution circuitry was used to safely control the mechanical components of the test stand. Control circuitry combined with Lab View was used to provide local/remote control of the test stand during operation.

We ran out of time to complete the debugging phase of the test stand project. All electrical components have been acquired and hardware assembly has been completed. Successful signal generation of the FDCS and CI waveforms from the field point modules remains to be completed.

This project is a continuation of the "Fuel Injector Test Stand" project from Fall 2002. The goal of this phase of the project is to reverse engineer the fuel injector driver module, which governs the operation of the injectors, and then to implement the test stand in the laboratory with the use of electronic controls. The previous group installed the main mechanical hardware components. These systems will need to be tested together with the current project so that steady state operation system data can be collected to establish how the system works. Eventually data will also be collected from the injectors. The following outlines the overall project deliverables:

- Fuel Injector Driver Control System
- Integration of all components of the fuel injector test stand
- Steady state operational data from the test stand
- Description of how to instruct a person to operate the stand and systems
- Weekly report of team and individual decisions and activities, including a running list of open questions and issues to be addressed

The power distribution system is designed to fulfill the following goals:

- Distribute 240V single phase AC to the oil pump, gas pump and oil heater and 120V AC to the fuel cooling fans and the 12VDC 50A power supply
- Provide an automatic shutdown of the system and solenoid controlled pneumatic valves to shut off the fuel supply if one of the following conditions are met:
    - A low-pressure signal is received on one of the pumps in Lab View
    - The panic button is pressed at either the test stand itself or from the Lab View control panel
- Maintain design simplicity

The distribution system also provides over current protection and ensures that each load has to be manually restarted after an automatic trip. In addition to a hardware control panel, the Lab View program will be used to control the system through a virtual control panel.

The distribution system was broken down into three parts: an AC section, a control section, and a control panel. The AC section is the load distribution section consisting of a breaker and a 120V AC controlled contactor to act as an on/off switch for each of the loads. Front panel switches, the Lab View control panel, and the safety shutdown system operate the contactors.

The purpose of the control panel is to allow local and remote operation of the test bench. The control panel is broken down into two types of circuits. Each circuit contains a momentary switch, a 12V DC single pole relay, and an N type MOSFET.

The control panel has inputs from the 12V DC power supply and switching signals from the Lab View program via the field point modules. The output of the control panel is a 120VAC signal, which controls the respective control relay in the control box.

The test bench has 5 loads: the oil pump, the oil heater, the fuel pump, the fuel cooler fans, and the safety circuit. Each load has a start/reset button and a stop/emergency stop button. The

start/reset and stop switches are located on the covers of the control boxes. The emergency stop switch is a momentary break switch and is located around the corner from the test bench.

Figure 31 shows a block diagram of the fuel injector driver control system.

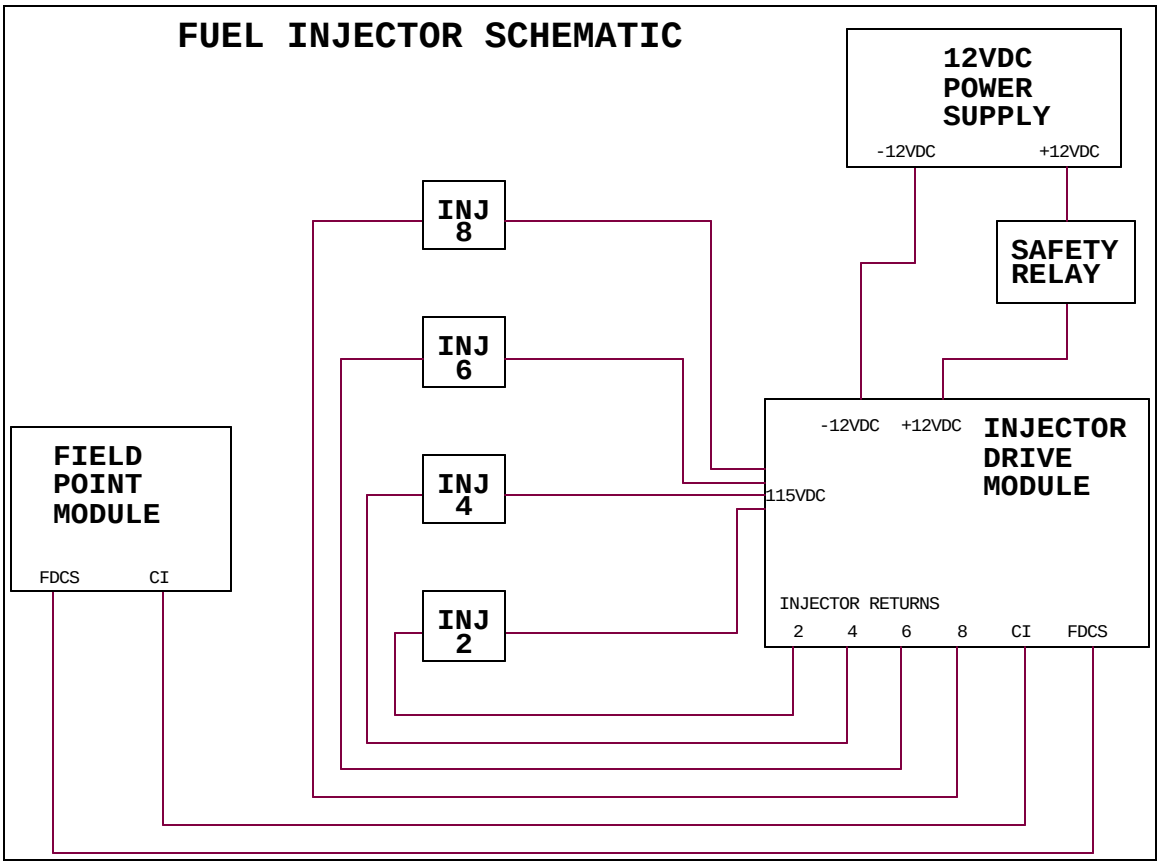

Fig. 31. Fuel Injector Driver Control System

The control system contains all of the controls and a safety circuit. This system consists of a 12VDC 50 Amp power supply and a 120VAC control voltage bus. Lab View is used to control the firing of the fuel injectors as well as operate safety features built into the control system. Figure 32 shows a diagram of the control system.

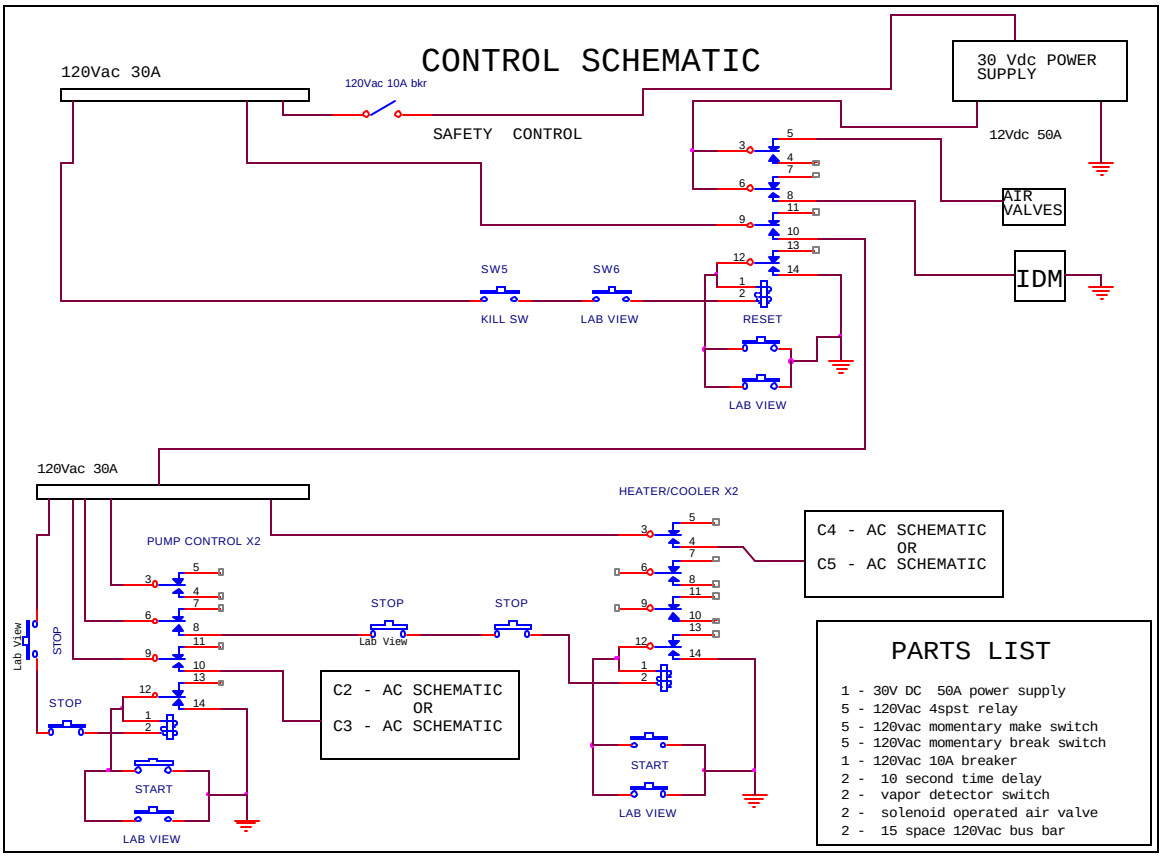

Fig. 32. Test Stand Control System

The 120VAC control voltage has to go through the safety circuit first. The coil of the safety circuit is connected to the 120VAC control voltage bus. In line with the safety relay coil are the vapor detector contacts, the oil and gas low-pressure switches, and the local and Lab View panic safety switches. The coil also goes through one of the contacts of the relay to ensure that the system does not re-energize once the trip condition clears. The circuit can be re-energized by using either reset switch.

Summary

The EE 403W design team was issued the challenge of designing and creating a power distribution and control system for our sponsor, Energy Institute. The driving force behind this project was the need to test the durability of diesel engine fuel injectors using Dimethyl Ether fuel blends.

The design team was responsible for the successful completion of the fuel injector driver module control system, and the integration of the fuel injector test stand from an electrical standpoint. We used a combination of hardware design and software implementation to integrate all components of the fuel injector test stand.

Our design solution has both hardware and software features. The hardware aspects of the design solution include a safety relay circuit to ensure proper operation of the test stand as well

as a local control panel. The software side employs Lab View to remotely control the test stand operation and to collect the desired pressure/temperature data through the field point modules.

We were unable to finish the test stand project in the time allotted, but future work should be minimal and easy to complete. All hardware components have been assembled. Successful signal generation of the FDCS and CI waveforms from the field point modules remains to be completed.

Present Status of the Fuel Injector Test Stand

CONCLUSION

The work summarized here for Tasks 1 and 2 of the project lead to the following conclusions.

1. While lubricity additives has been shown to yield adequate lubricity to DME when blended at sufficient concentration (see the work of Sivebaek et al.), these lubricity additives do not provide sufficient improvement to the viscosity of DME to alleviate the wear-related problems of DME. An effective viscosity improver is still needed.

2. The Cameron-Plint wear test apparatus has confirmed the modes of wear that can occur with DME blended fuels.

Blending DME in diesel fuel is one option to utilize DME in diesel engines without drastic redesign of fuel pumps and fuel injectors. However, even modest addition of DME into diesel fuel significantly reduces the viscosity of the fuel mixture. Addition of as little as 25 wt.% DME into diesel fuel reduces fuel viscosity below the ASTM specification. This suggests that viscosity rather than miscibility is the limiting factor in blending DME with diesel fuel. Examination of other, more viscous substances, blended with DME showed that additization alone is unlikely to accomplish the goal of raising the viscosity of DME to the level of conventional fuels. Neither vegetable oil fuels or lubricity additives increased the level of fuel viscosity to that of diesel fuel without blending at levels above 50 wt.% in DME. Therefore, either new compounds specifically designed to provide a viscosity improvement must be formulated, or fuel blending will be required to achieve diesel-like fluid properties. Lubricity may be enhanced through the use of surface film forming additives.

ACKNOWLEGDMENT

The authors wish to acknowledge the support of Air Products and Chemicals, Inc., Caterpillar, Inc., Ethyl Additives, Inc., the Pennsylvania Department of Environmental Protection and the National Energy Technology Laboratory of the U.S. Department of Energy. In particular, the authors wish to acknowledge the support and encouragement of John Winslow, Mike Nowak and Jenny Tennant of NETL and Barry Halper, Jo Ann Franks and Jim Sorensen of Air Products, and especially Peter J.A. Tijm (formerly of Air Products).

The authors wish to thank and acknowledge donation of additives for use in this project by Ethyl Additives, Inc. and Lubrizol, Inc. Also, the authors wish to thank Elana Chapman for directing the selection of additives considered in this work and for her collaboration on the project.

The authors wish to acknowledge their gratitude and appreciation for the efforts of our departed colleague, Dr. Joeseph Conway, who contributed greatly to the success of this project.

This paper was written with support of the US Department of Energy under Contract no. DE-FG29-99FT40161 and Cooperative Agreement DE-FC26-01NT41115. The Government reserves for itself and others acting on its behalf a royalty-free, nonexclusive, irrevocable,

This material was prepared with the support of the Pennsylvania Department of Environmental Protection. Any opinions, findings, conclusions, or recommendations expressed herein are those of the author(s) and do not necessarily reflect the views of the DEP.

REFERENCES

[1] Eirich, J., E. Chapman, H. Glunt, D. Klinikowski, A.L. Boehman, J.G. Hansel and E.C. Heydorn, "Development of a Dimethyl Ether (DME)-Fueled Shuttle Bus," **2003**, Society of Automotive Engineers Technical Paper No. 2003-01-0756.

[2] Bhide, S., D. Morris, J. Leroux, K.S. Wain, J.M. Perez and A.L. Boehman. Characterization of the Viscosity of Blends of Dimethyl Ether with Various Fuels and Additives. **2003**, *Energy & Fuels*, **17**, 1126-1132.

[3] Fleisch, T., McCarthy, C., Basu, A., Udovich, C., Charbonneau, P., Slodowske, W., Mikkelson, S.-E., and McCandless, J., "A New Clean Diesel Technology: Demonstration of ULEV Emissions on a Navistar Diesel Engine Fueled with Dimethyl Ether," **1995**, Society of Automotive Engineers Technical Paper No. 950061.

[4] Kapus, P. E., and Cartellieri, W. P., "ULEV Potential of a DI/TCI Diesel Passenger Car Engine Operated on Dimethyl Ether," **1995**, Society of Automotive Engineers Technical Paper No. 952754.

[5] Karpuk, M. E. and Cowley, S. W., "On Board Dimethyl Ether Generation to Assist Methanol Engine Cold Starting," **1988**, Society of Automotive Engineers Technical Paper No. 881678.

[6] Green, C. J., Cockshutt, N. A. and King, L., "Dimethyl Ether as a Methanol Ignition Improver: Substitution Requirements and Exhaust Emissions Impact," **1990**, Society of Automotive Engineers Technical Paper No. 902155.

[7] Murayama, T., Chikahisa, T., Guo, J., and Miyano, M., "A Study of a Compression Ignition Methanol Engine with Converted Dimethyl Ether as an Ignition Improver," **1992**, Society of Automotive Engineers Technical Paper No. 922212.

[8] Guo, J., Chikahisa, T., Murayama, T., and Miyano, M., "Improvement of Performance and Emissions of a Compression Ignition Methanol Engine with Dimethyl Ether," **1994**, Society of Automotive Engineers Technical Paper No. 941908.

[9] Hansen, J. B., Voss, B., Joensen, F., and Siguroardottir, I. D., "Large Scale Manufacture of Dimethyl Ether – a New Alternative Diesel Fuel from Natural Gas," **1995**, Society of Automotive Engineers Technical Paper No. 950063.

[10] Wilson, R., "DME Shows Promise as Drop-In 'Replacement' for Diesel Fuel; Tests Meet CARB 1998 ULEV Standards," **1995**, *Diesel Progress Engines and Drives*, June 1995, pp. 108-109.

[11] Fleisch, T. H., "More on Dimethyl Ether: Case is Building for DME as Clean Diesel Fuel," *Diesel Progress Engines and Drives*, **1995**, October 1995, pp. 42-45.

[12] Glensvig, M., Sorenson, S. C. and Abata, D. L., "An Investigation of the Injection Characteristics of Dimethyl Ether," **1997**, ASME Paper No. 97-ICE-67, ICE-Vol. 29-3, pp. 77-84.

[13] McCandless, J. C. and Li, S., "Development of a Novel Fuel Injection System (NFIS) for Dimethyl Ether – and Other Clean Alternative Fuels," **1997**, Society of Automotive Engineers Technical Paper No. 970220.

[14] Alam, M., Fujita, O., Ito, K., Kajitani, S., Oguma, M. and Machida, H., "Performance of NOx Catalyst in a DI Diesel Engine Operated with Neat Dimethyl Ether," **1999**, Society of Automotive Engineers Technical Paper No. 1999-01-3599.

[15] Sorenson, S. C., and Mikkelsen, S.-V., "Performance and Emissions of a 0.273 Liter Direct Injection Diesel Engine Fuelled with Neat Dimethyl Ether," **1995**, Society of Automotive Engineers Technical Paper No. 950064.

[16] Kapus, P. and Ofner, H., "Development of Fuel Injection Equipment and Combustion System for DI Diesels Operated on Dimethyl Ether," **1995**, Society of Automotive Engineers Technical Paper No. 950062.

[17] Longbao, Z., Hewu, W., Deming, J., Zuohua, H., "Study of Performance and Combustion Characteristics of a Dme- Fueled, Light-Duty, Direct-Injection Diesel Engine," **1999**, Society of Automotive Engineers Technical Paper No. 1999-01-3669.

[18] Kajitani, S., Chen, Z.L., Konno, M., Rhee, K.T., "Engine Performance and Exhaust Characteristics of Direct Injection Diesel Engine Operated with DME" **1997**, Society of Automotive Engineers Technical Paper No. 972973.

[19] Christensen, R., Sorenson, S.C., Jensen, M.G., Hansen, K.F., "Engine Operation on Dimethyl Ether in a Naturally Aspirated IDI Diesel Engine," **1997**, Society of Automotive Engineers Technical Paper No. 971665.

[20] DuPont Fluorochemicals, "DuPont Dymel®A Aerosol Propellants, Fluorochemicals Laboratory," E. I. duPont de Nemours and Company, ATB-25, www.dupont.com/dymel.

[21] Chapman, E. M, Bhide, S. V., Boehman, A. L., Tijm, P. J. A. and Waller, F. J., "Emission Characteristics of a Navistar 7.3L Turbodiesel Fueled with Blends of Oxygenates and Diesel," **2000**, Society of Automotive Engineers Technical Paper No. 2000-01-2887.

[22] Chapman, E.M., Boehman, A.L., Tijm, P.J.A. and Waller, F.J., "Emission Characteristics of a Navistar 7.3L Turbodiesel Fueled with Blends of Dimethyl Ether and Diesel Fuel," **2001**, Society of Automotive Engineers Technical Paper No. 2001-01-3626.

[23] Eirich, J., Chapman, E., Glunt, H., Klinikowski, D., Boehman, A. L., Hansel, J. G. and Heydorn, E. C., "Development of a Dimethyl Ether (DME)-Fueled Shuttle Bus," **2003**, Society of Automotive Engineers Technical Paper No. 2003-01-0756.

[24] American Society for Testing of Materials, "D975-98b Standard Specification for Diesel Fuel Oils", 2000 Annual Book of ASTM Standards: Petroleum Products, Lubricants, and Fossil Fuels, Volume 05.01, West Conshohocken, PA (2000).

[25] Sivebaek, I. M., Sorenson, S. C., and Jakobsen, J., "Dimethyl Ether (DME) – Assessment of Viscosity Using the New Volatile Fuel Viscometer (VFVM)," **2001**, Society of Automotive Engineers Technical Paper No. 2001-01-2013.

[26] Teng, H., McCandless, J. C., and Schneyer, J. B., "Thermochemical Characteristics of Dimethyl Ether – An Alternative Fuel for Compression-Ignition Engines," **2001**, Society of Automotive Engineers Technical Paper No. 2001-01-0154.

[27] Kershner, D., Morris, D., Boehman, A., Perez, J. M., and Sharer, D., "Investigation of Raw Soy Oil as a Diesel Fuel Extender" Proceedings, AOCS International Meeting, Istanbul, Turkey, May **2002.**

[28] Song, J., K. Cheenkakorn, J. Wang, J. Perez, A.L. Boehman, P.J. Young and F.J. Waller. "Effect of Oxygenated Fuel on Combustion and Emissions in a Light-Duty Turbo Diesel Engine," **2002**, *Energy & Fuels*, **16**, 294-301.

[29] Wain, K.S., and Perez, J.M., "Oxidation of Biodiesel Fuels for Improved Lubricity", **2002**, ASME 2002-ICE-447, ICE-Vol. 38, pp. 27-34**.**

[30] Johnson, R.H., "Design and Use of a Precision Pressure Viscometer," **1962**, M.S. Thesis, The Pennsylvania State University, University Park, PA.

[31] American Society for Testing of Materials, "D445-97 Standard Test Method for Kinematic Viscosity of Transparent and Opaque Liquids (the Calculation of Dynamic Viscosity)", 2000 Annual Book of ASTM Standards: Petroleum Products, Lubricants, and Fossil Fuels, Volume 05.01, West Conshohocken, PA (2000).

[32] Wain, K., Ph.D. Thesis, **2004**, Department of Chemical Engineering, The Pennsylvania State University.

[33] American Society for Testing of Materials, "D341-93(1998) Standard Viscosity-Temperature Charts for Liquid Petroleum Products", 2000 Annual Book of ASTM Standards: Petroleum Products, Lubricants, and Fossil Fuels, Volume 05.01, West Conshohocken, PA (2000).

[34] Sivebaek, I.M. and Sorenson, S.C., "Dimethyl Ether (DME) – Assessment of Lubricity Using the Medium Frequency Pressurised Reciprocating Rig Version 2 (MFPRR2)," **2000**, Society of Automotive Engineers Paper No. 2000-01-2970.

[35] Nielsen, K. and Sorenson, S.C., "Lubricity Additives and Wear with DME in Diesel Injection Pumps," **1999**, ASME Paper 99-ICE-217, ICE-Vol. 33-1, pp. 145-153.

[36] Chapman, E., M.S. Thesis, "Optimization of a Diesel Engine for Operation on Blends of Dimethyl Ether / Diesel Fuel Blends," **2002**, Fuel Science Program, Department of Energy & Geo-Environmental Engineering, The Pennsyvlania State University.